AD-A282 902

AD

TECHNICAL REPORT ARCCB-TR-94019

NUMERICAL BOX-COUNTING AND CORRELATION INTEGRAL MULTIFRACTAL ANALYSIS

44 Pj 94-24645

L.V. MEISEL
M.A. JOHNSON

MAY 1994

US ARMY ARMAMENT RESEARCH,
DEVELOPMENT AND ENGINEERING CENTER
CLOSE COMBAT ARMAMENTS CENTER
BENÉT LABORATORIES
WATERVLIET, N.Y. 12189-4050

94 8 03 048

DISCLAIMER

The findings in this report are not to be construed as an official Department of the Army position unless so designated by other authorized documents.

The use of trade name(s) and/or manufacturer(s) does not constitute an official indorsement or approval.

DESTRUCTION NOTICE

For classified documents, follow the procedures in DoD 5200.22-M, Industrial Security Manual, Section II-19 or DoD 5200.1-R, Information Security Program Regulation, Chapter IX.

For unclassified, limited documents, destroy by any method that will prevent disclosure of contents or reconstruction of the document.

For unclassified, unlimited documents, destroy when the report is no longer needed. Do not return it to the originator.

REPORT DOCUMENTATION PAGE

Form Approved
OMB No. 0704-0188

1. AGENCY USE ONLY *(Leave blank)*

2. REPORT DATE
May 1994

3. REPORT TYPE AND DATES COVERED
Final

4. TITLE AND SUBTITLE
NUMERICAL BOX-COUNTING AND CORRELATION INTEGRAL MULTIFRACTAL ANALYSIS

5. FUNDING NUMBERS
AMCMS: 6126.24.H180
PRON: 470TEV64471A

6. AUTHOR(S)
L.V. Meisel and M.A. Johnson

7. PERFORMING ORGANIZATION NAME(S) AND ADDRESS(ES)
U.S. Army ARDEC
Benét Laboratories, SMCAR-CCB-TL
Watervliet, NY 12189-4050

8. PERFORMING ORGANIZATION REPORT NUMBER
ARCCB-TR-94019

9. SPONSORING/MONITORING AGENCY NAME(S) AND ADDRESS(ES)
U.S. Army ARDEC
Close Combat Armaments Center
Picatinny Arsenal, NJ 07806-5000

10. SPONSORING/MONITORING AGENCY REPORT NUMBER

11. SUPPLEMENTARY NOTES
Submitted to: *Journal of Computational Physics*

12a. DISTRIBUTION/AVAILABILITY STATEMENT

Approved for public release; distribution unlimited

12b. DISTRIBUTION CODE

13. ABSTRACT *(Maximum 200 words)*
A systematic study of the rate of convergence, cpu time, and accuracy of a numerical box-counting and a numerical correlation integral algorithm to Euclidean point sets, Koch constructions, and a symmetric chaotic mapping is described.

14. SUBJECT TERMS
Fractals, Multifractal Measures, Box-Counting Algorithms, Correlation Integral Methods, Numerical Multifractal Analysis

15. NUMBER OF PAGES
38

16. PRICE CODE

17. SECURITY CLASSIFICATION OF REPORT	18. SECURITY CLASSIFICATION OF THIS PAGE	19. SECURITY CLASSIFICATION OF ABSTRACT	20. LIMITATION OF ABSTRACT
UNCLASSIFIED	UNCLASSIFIED	UNCLASSIFIED	UL

TABLE OF CONTENTS

Tables

List of Illustrations

INTRODUCTION

Recently, F.H. Ling and G. Schmidt (ref 1) argued that box-counting techniques are superior to the Grassberger-Procaccia (correlation integral) algorithm (ref 2) for dealing with experimental data sets.

Reference 1 applied a box-counting method to determine the capacity dimension D(0), information dimension D(1), and correlation dimension D(2) of the attractors of the Henon map, the logistic map, the Lorentz equation, and to the attractor of pulsar 0950+08. They also used the conventional Grassberger-Procaccia method (i.e., the correlation integral method specialized to the determination of the correlation dimension) to the same data sets. The box-counting algorithm of Reference 1 is similar to that of Block, Bloh, and Schellnhuber (ref 3) in that only data concerning occupied boxes are stored and analyzed.

The box-counting and correlation integral algorithms of Reference 1 yielded fractal dimensions within about 3 percent of analytic values for the logistics map (using a 1000 point sample), Henon map (2000 points), and Lorentz equation (4000 points) for embedding dimensions $\geq$ 1, 2, and 3, respectively. Restricted point sets were employed to reflect the fact that experimental point sets are generally limited to similar ranges. Reference 1 concluded that 4000 points are sufficient for the determination of D(0), D(1), and D(2) of the fractal attractor of pulsar 0950+08. The pulsar dimensions have values near 5 and were determined in a 14 dimensional embedding space.

Reference 1 asserts that most authors use the correlation dimension as the "main measure" of a strange attractor. They also conclude that box-counting algorithms require less computation time and yield results at least as good as those obtained using the Grassberger-Procaccia method for the correlation dimension. Therefore, Ling and Schmidt (ref 1) conclude that box-counting is superior to the Grassberger-Procaccia algorithm. However, they also note that the Grassberger-Procaccia algorithm is "superior" to box-counting for determining the capacity dimension.

Although Ling and Schmidt (ref 1) are particularly interested in algorithmic speed, they also address a very important issue concerning multifractal measurement, viz., How large a data set is needed to obtain a reasonable approximation to the fractal measures of interest in a given case?

It may well be the case that for highly complex chaotic dynamical systems (such as that underlying the observations of pulsar 0950+08), the best one can hope to do is to determine D(0), D(1), and D(2). However, there are numerous cases (for example, diffusion limited aggregation) where the determination of D(q) for general q is important. This report describes a systematic approach, over extensive ranges of q, to the question of convergence for box-counting and correlation integral-based multifractal analysis.

THEORY

The expression for the box-counting (Hentschell-Procaccia) generalized dimension D(q) in a d dimensional topological space is

$$(q-1)D(q) = \lim_{E \to 0} \frac{\ln\left(\sum_{i=1}^{N(E)} P_i^q(E)\right)}{\ln(E)}, \qquad q \neq 1,$$

where in the summation i runs over N(E) occupied d dimensional hypercubes (boxes) of edge length E and $P_i(E)$ is the probability of finding a point of the fractal set in the i^{th} box. As implicitly stated in Eq. (1) of Reference 1 and demonstrated for a number of cases in Reference 4, box-counting algorithms do not converge for q<0 in many cases. In practice, one deals with finite subsets of the fractal set and determines a numerical approximation to (q-1)D(q) by fitting

$$\ln\left(\sum_{i=1}^{N(E)} P_i^q(E)\right) = (q-1)D(q)\ln(E) + Const$$

over an "appropriate" range of E values.

The generalized correlation integral is defined as

$$C(q,E) = \lim_{N \to \infty} \frac{1}{N}\sum_{i}^{N} \left[\frac{1}{N}\sum_{j}^{N} H(E - |x_i - x_j|)\right]^{q-1}, \quad q \neq 1$$

where at each stage in the limit process $\mathbf{x}_i$ and $\mathbf{x}_j$ (d dimensional vectors) run over the N element fractal subset and H(x) is the Heaviside function. The Hentschell-Procaccia fractal dimension D(q) is determined by

$$(q-1)D(q) = \lim_{E \to 0^+} \frac{\ln(C(q,E))}{\ln(E)}$$

In practice, one deals with finite subsets of the fractal set and determines a numerical approximation to (q-1)D(q) by fitting over a range of E, etc., as in box counting. (Usually a Euclidean metric is assumed for determining $|\mathbf{x}_i - \mathbf{x}_j|$. Frequently, the outer summation in the expression for C(q,E) is taken over a subset, a reference set, of the fractal subset.)

RESULTS AND DISCUSSION

Results were obtained for two specific numerical algorithms:

1. The agglomeration box-counting (ABC) algorithm (ref 4) represents box-counting algorithms. The results of standard "sorting" box-counting algorithms (for relatively smaller ranges of N) at all q were consistent with the results obtained via ABC for the models reported in Reference 4.

2. The box-based correlation integral (BBCI) method (ref 5) provides the numerical realization of the correlation integral method. BBCI converged near analytic values in all cases.

These algorithms are well suited to the analysis of large data sets and are therefore well suited to convergence studies. ABC and BBCI would require modifications to efficiently handle relatively sparse data in high dimensional spaces.

The model point sets studied include Euclidean sets, Koch asymmetric [0.4,0.2] and symmetric triadic snowflakes (ref 6), split snowflake halls (ref 7), the 13 element generator Koch construction (ref 8) discussed in Reference 6, and the attractor for the sixfold (D6) symmetric chaotic mapping of Figure 3 of Reference 9.

The algorithms were applied to identical model data for each N. The multifractal data were stored in 768x768 box arrays, which simulate image acquisition data. The initiators of the Koch constructions (ref 6) were randomly oriented with respect to the axes of the box array. The boxes, in which the data to be analyzed were stored, were designated "elementary boxes." For the point sets studied, Reference 4 demonstrated that as the number of elementary boxes increases, converged values tend to be closer to analytic values, but the number of points required for convergence increases.

Figures 1 through 5 present a selection of results of applying the box-counting algorithm (ABC) and the correlation integral algorithm (BBCI) for specific fractal models and specific q values. The graphs display measured D(q) versus a range of normalized ln(N). Each graph shows open circles representing measured values connected by lines. If available, the analytic value of D(q) is shown as a horizontal line.

Table 1 summarizes convergence results for the five model fractal sets. We refer to "converged" results as those within 1 percent of the values obtained at the largest N and "good" results as those within 5 percent. Converged values may differ from analytic values by more than 1 percent. Values of N sufficient to obtain converged results are denoted N_1 and good results N_5. The range of N for 5 percent (or 1 percent) convergence extends below the value of N_5 (or N_1) in the table. It falls between N_5 (or N_1) and the next lower N point.

The definition of "good" convergence is arbitrary. Multifractal measures converged within 20 percent might be important. One should not conclude that N_5 is a minimum number of points for application of multifractal analysis. Table 1 or the figures serve as guides for the application of box-counting and/or correlation integral algorithms.

The ABC algorithm converges to values near those of BBCI at all q for the Euclidean point sets and the sixfold symmetric chaotic mapping; ABC diverges for $q<0$ for the other fractal point sets.

BBCI overshoots and converges from above for the triadic snowflake (monofractal) and the sixfold symmetric mapping. All other convergent cases approach their limits from below.

With the exception of the monofractal triadic snowflake, ABC and BBCI converge at about the same rate at $q>=0$. BBCI requires nearly ten times as many points at $q<0$ than at $q>=0$ to obtain good results.

Where analytic measures are known, BBCI results are closer than ABC. The model fractal sets having D(0) near 1.2 require about 10^3 points to yield good convergence at all q. Those having D(0) near 2.0 require between 10^4 and 10^5 points at $q \geq 0$ and between 10^5 and about 10^6 points at $q<0$ for good convergence.

Figure 6 shows ABC and BBCI cpu time versus normalized ln(N) for the fractal models. BBCI cpu time exceeds ABC cpu time for large N, but it is lower at small N. The curves cross between 10^3 and 10^4. Both of the present algorithms generally yield good (5 percent) convergence for N between 10^3 and 10^5 at $q>0$.

Cpu time tends to saturate for the present box-based algorithms, which are specialized to deal with occupation data in prescribed arrays. For exact coordinate data and the corresponding algorithms, cpu time will go like N^2 for correlation integral methods and like N ln(N) for sorting-based box-counting algorithms.

The size of the reference set, the number of shells in the fit, and the number of elementary boxes influence BBCI cpu time. Preliminary investigations suggest that a reference set comprised of 25 percent of the total number of points in the fractal subsets is sufficient to obtain equivalent results. The BBCI cpu times in Figure 6 were obtained using 100 percent of the points as a reference set and shell diameters ranging from 3 to 49. A 768x768 set of elementary boxes was used for both ABC and BBCI.

REFERENCES

1. F. H. Ling and G. Schmidt, *J. Comput. Phys.*, Vol. 99, 1992, p. 196.

2. P. Grassberger and I. Procaccia, *Phys. Rev. Lett.*, Vol. 50, 1983, p. 346; G. Paladin and A. Vulpiano, *Lett. Nuovo Cimento*, Vol. 41, 1984, p. 82; and K. Pawelzik and H.G. Schuster, *Phys. Rev. A*, Vol. 35, 1987, p. 481.

3. A. Block, W. von Bloh, and H.J. Schellnhuber, *Phys. Rev. A*, Vol. 42, 1990, p. 1869.

4. L.V. Meisel, Mark Johnson, and P.J. Cote, *Phys. Rev. A*, Vol. 45, 1992, p. 6989. We refer to the algorithm of Reference 4 as ABC.

5. Mark Johnson and L.V. Meisel, "Multifractal Analysis at Negative q," ARCCB-TR-92037, U.S. Army ARDEC, Benét Laboratories, Watervliet, NY, August 1992. We refer to the algorithm of Reference 5 as BBCI.

6. B.B. Mandelbrot, *Fractal Geometry of Nature*, Freeman, New York, 1983.

7. Ibid., p. 146. The level 3 version of this set is also known as the Monkey's Tree, see p. 31 of Ref. 6.

8. Ibid., p. 69.

9. M. Field and M. Golubitsky, *Computers in Physics*, Vol. 4, 1990, p. 470.

Table 1. Sufficient Values of N to Yield 1 Percent (N_1) and 5 Percent (N_5) Convergence. Box-Counting (ABC) Does Not Converge for q<0.

	\q	-25	-5	0	5	25
ABC	N_1			1.2E4	1.2E4	3.1E3
	N_5			3.1E3	770	770
asymmetric snowflake [0.4,0.2], D(0) = 1.16.						
BBCI	N_1	7.9E4	5.2E4	1.2E4	770	3.1E3
	N_5	3.1E3	3.1E3	770	190	770
ABC	N_1			1.2E4	1.2E4	5.2E4
	N_5			3.1E3	3.1E3	3.1E3
triadic snowflake, D(q) = 1.26 all q.						
BBCI	N_1	1.2E4	1.2E4	1.2E4	1.2E4	5.0E4
	N_5	770	770	770	770	770
ABC	N_1			1.8E6	1.6E5	1.6E5
	N_5			1.6E5	1.5E4	1.5E4
split snowflake halls, D(0) = 1.86.						
BBCI	N_1	2.4E9?	2.0E7	1.6E5	1.6E5	1.6E5
	N_5	1.6E5	1.6E5	1.5E4	1.5E4	1.5E4
ABC	N_1			3.7E5	3.7E5	3.7E5
	N_5			2.9E4	2.9E4	2.9E4
13 element generator, D(0) = 2.0.						
BBCI	N_1	8.2E8?	4.8E6	2.9E4	3.7E5	3.7E5
	N_5	4.8E6	3.7E5	2.9E4	2.9E4	2.2E3
ABC	N_1	1.0E9	1.0E9	1.0E6	1.0E5	1.0E6
	N_5	1.0E8	1.0E8	1.0E5	1.0E5	1.0E5
sixfold symmetric mapping, D(0) = 2.0.						
BBCI	N_1	1.0E7	1.0E7	1.0E6	1.0E5	1.0E6
	N_5	1.0E7	1.0E6	1.0E5	1.0E5	1.0E5

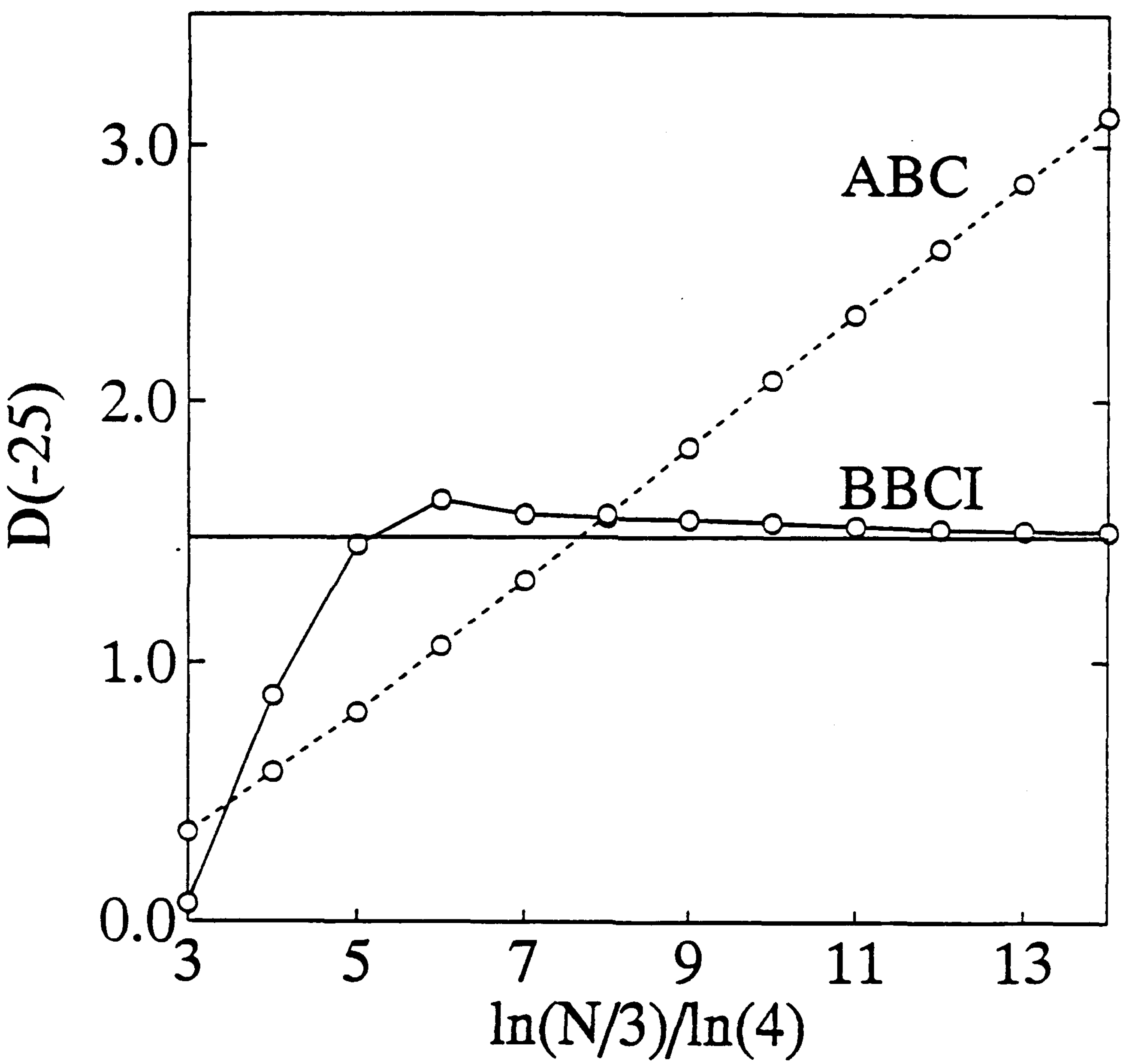

Figure 1. Hentschell and Procaccia generalized dimension D(q) versus normalized logarithm of the number of points in the fractal subset for the asymmetric [0.4,0.2] triadic snowflake.

(a). q = -25.

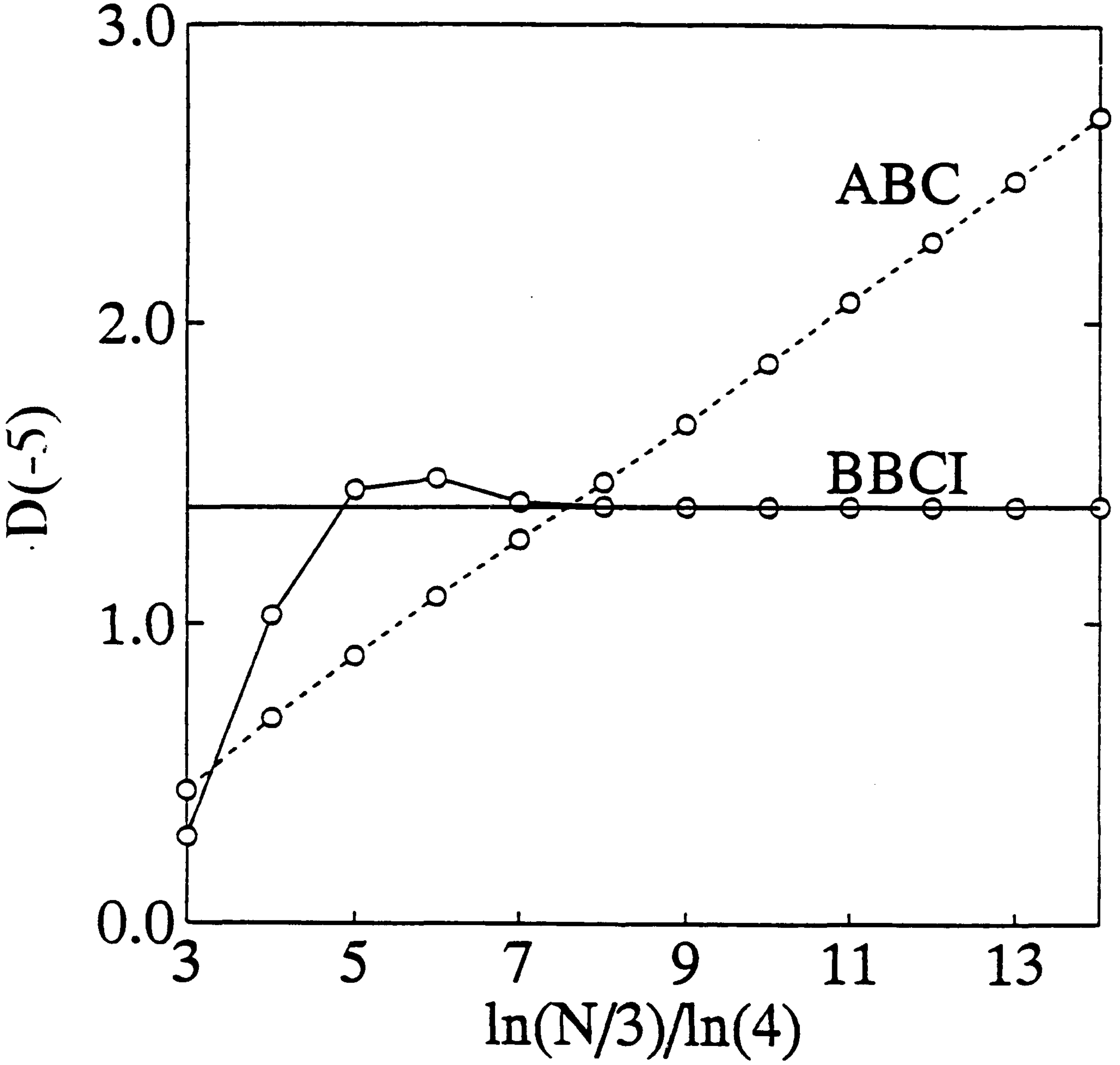

Figure 1(b). q = -5.

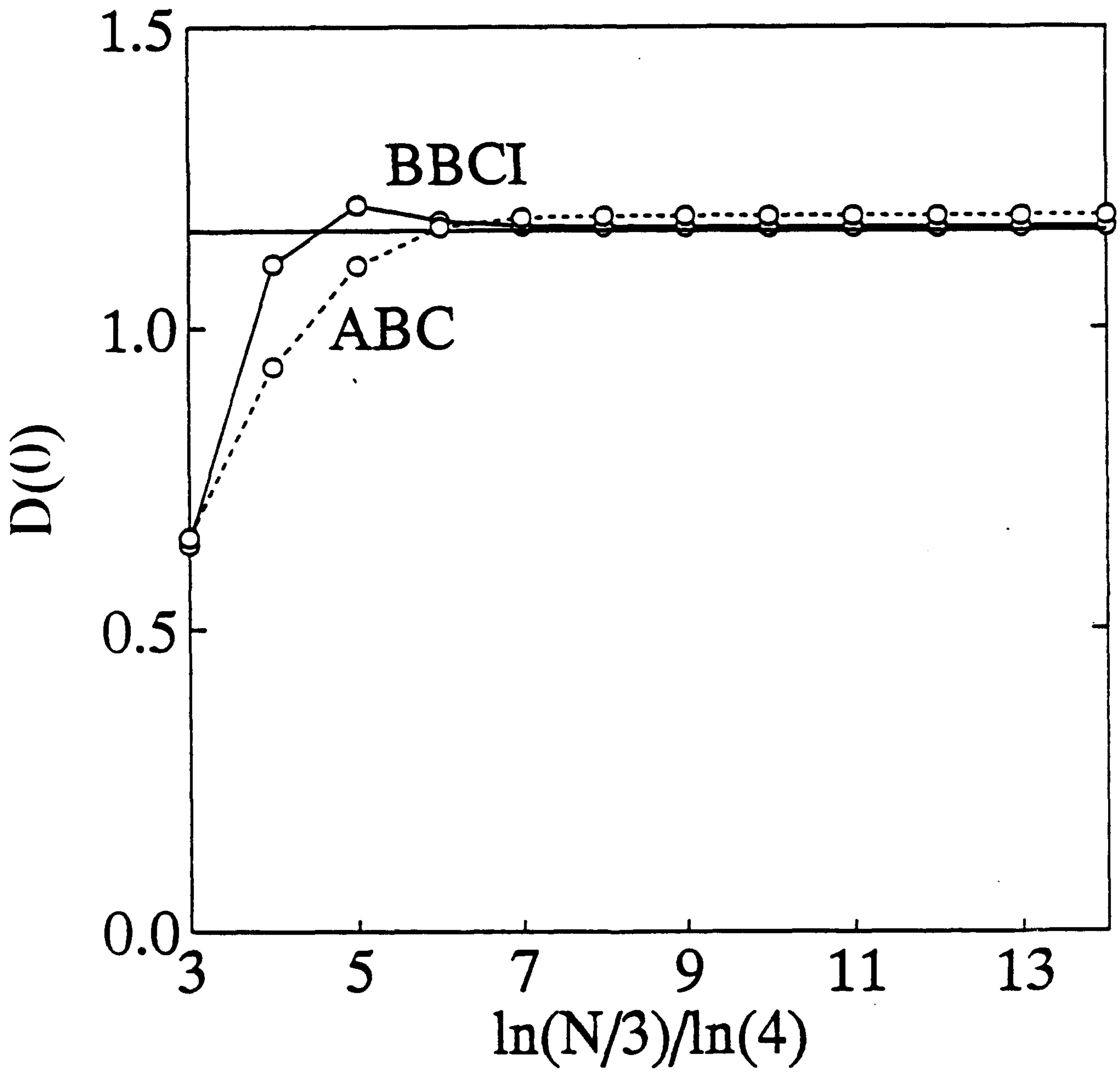

Figure 1(c). q = 0.

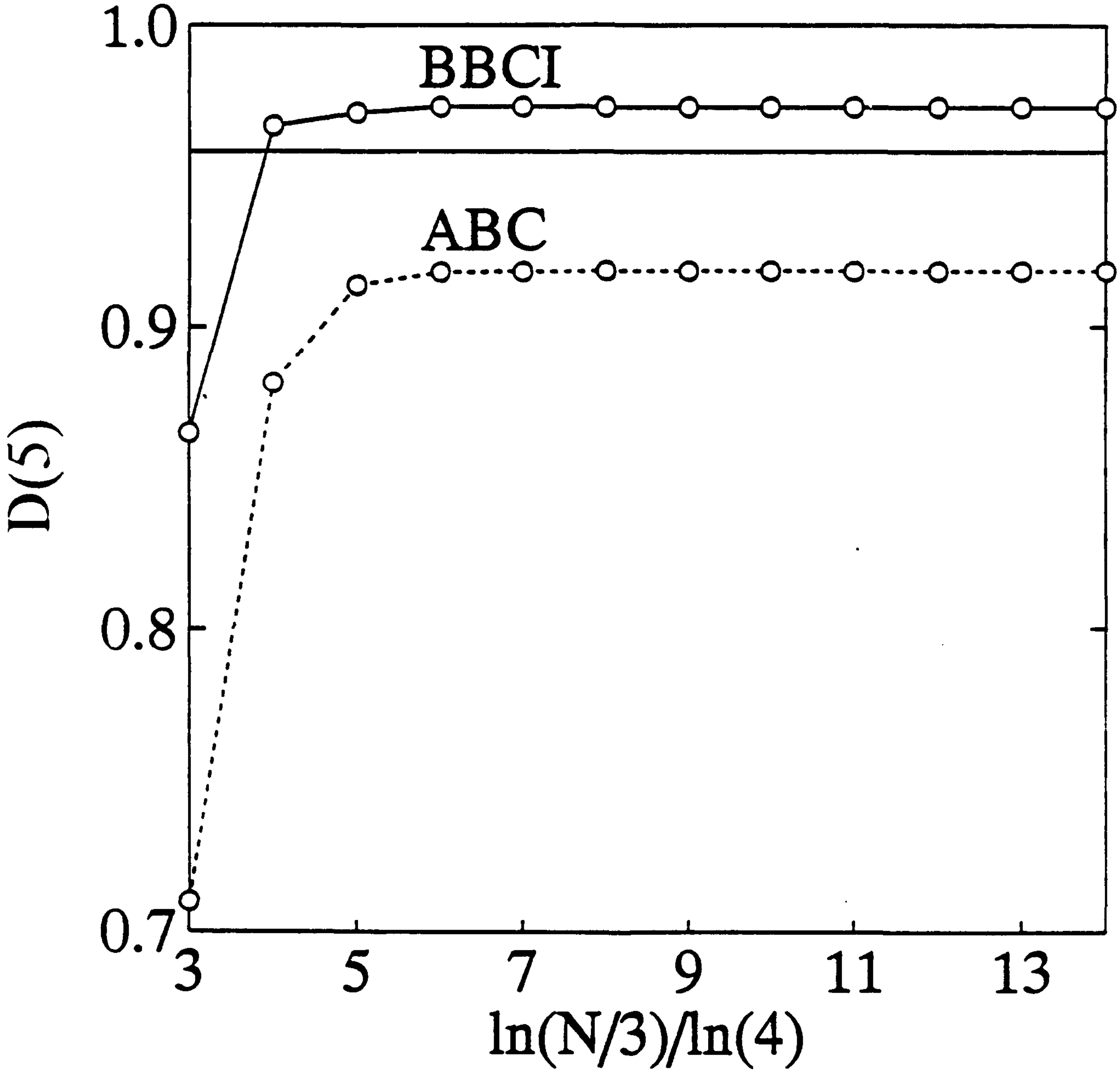

Figure 1(d). q = 5.

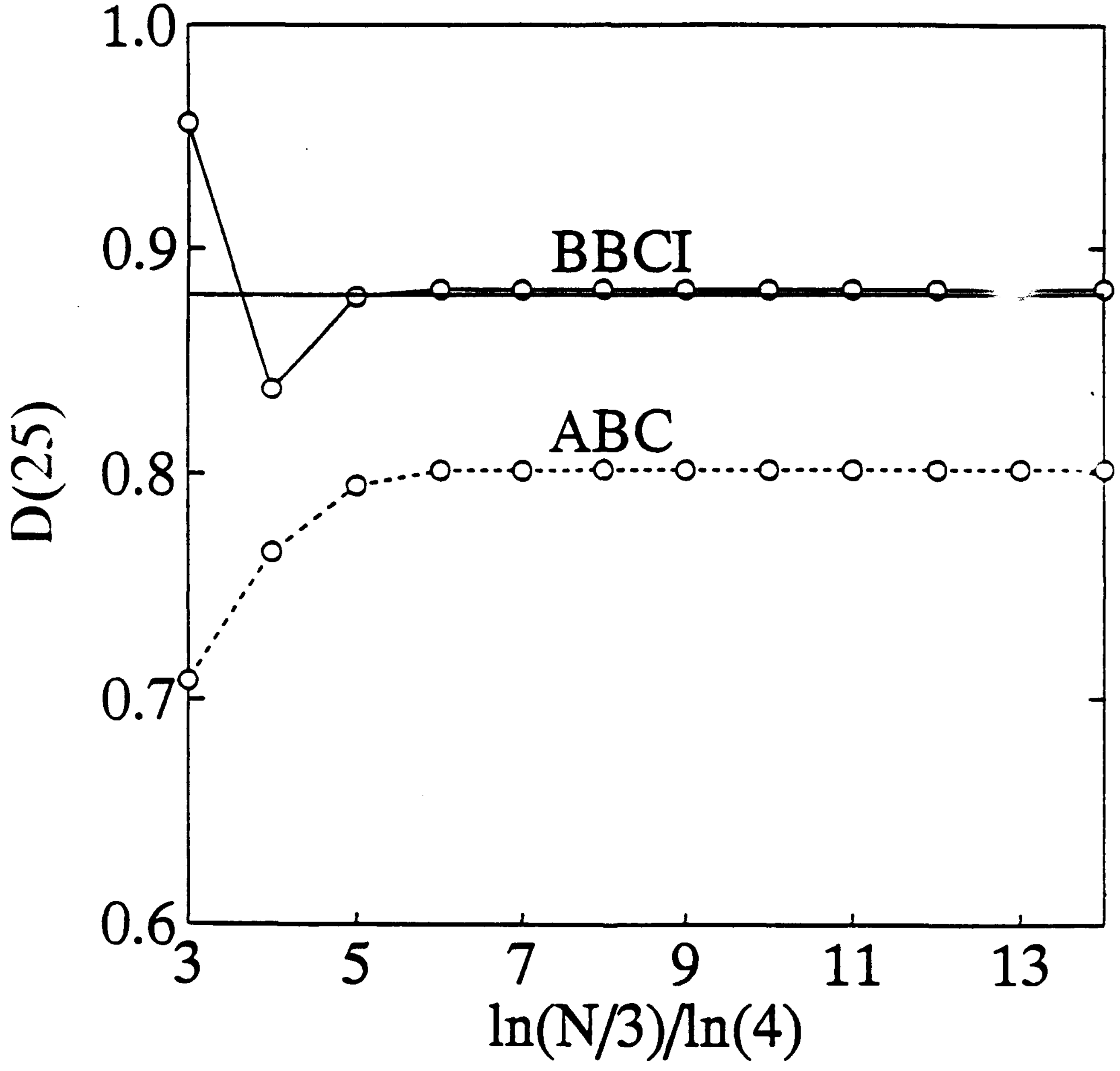

Figure 1(e). q = 25.

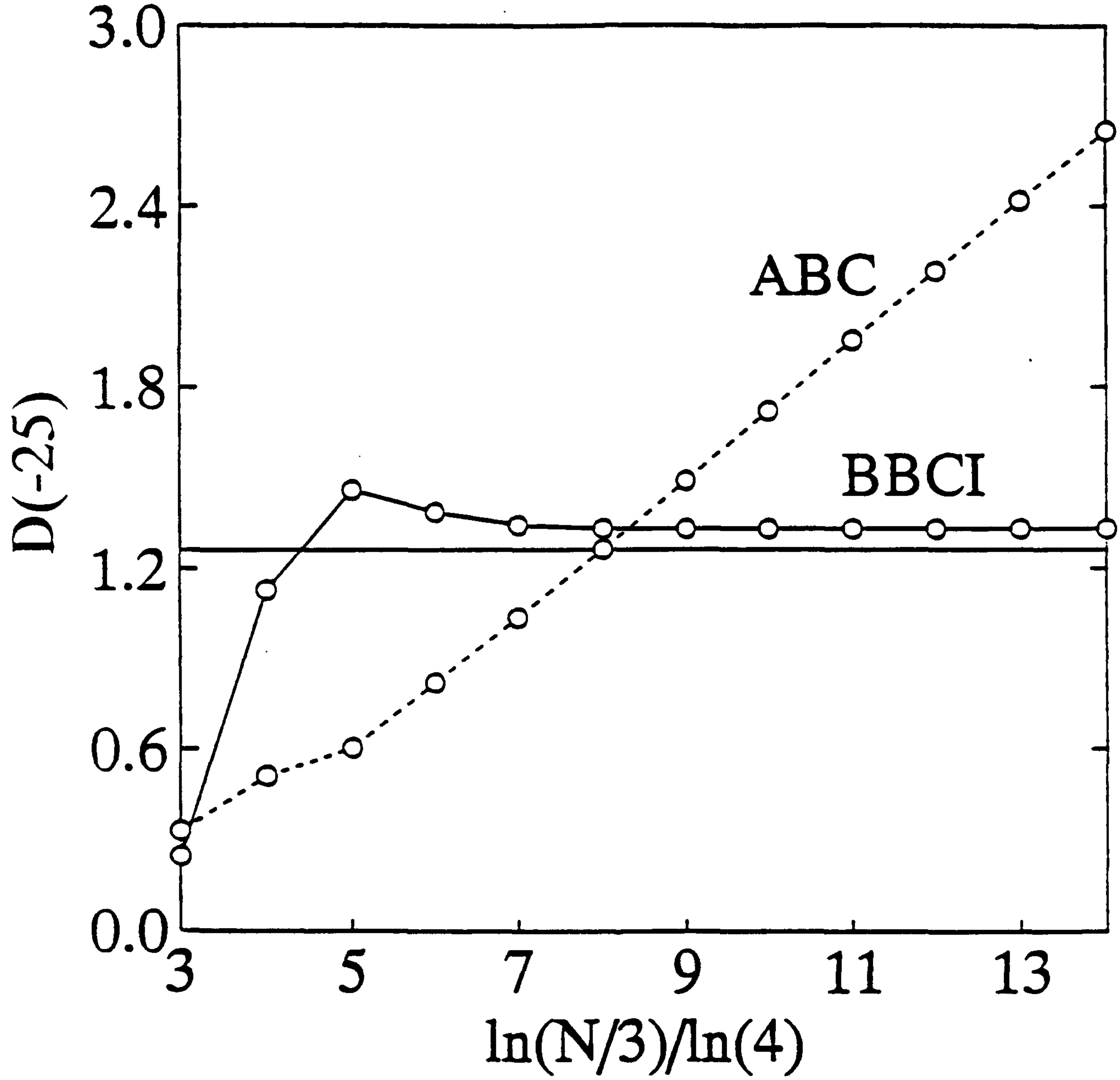

Figure 2. Hentschell and Procaccia generalized dimension D(q) versus normalized logarithm of the number of points in the fractal subset for the monofractal Koch triadic snowflake.

(a). q = -25.

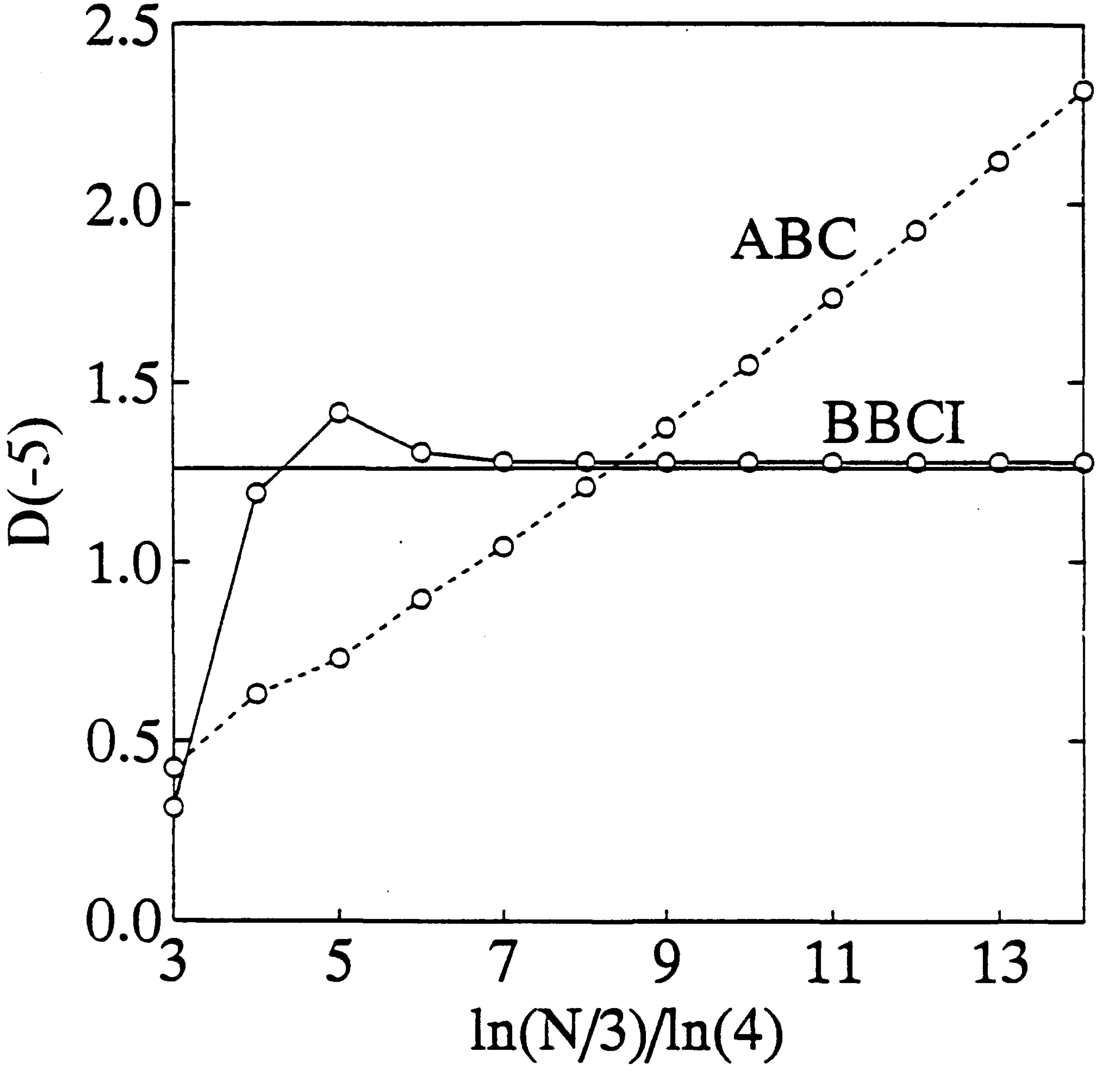

Figure 2(b). $q = -5$.

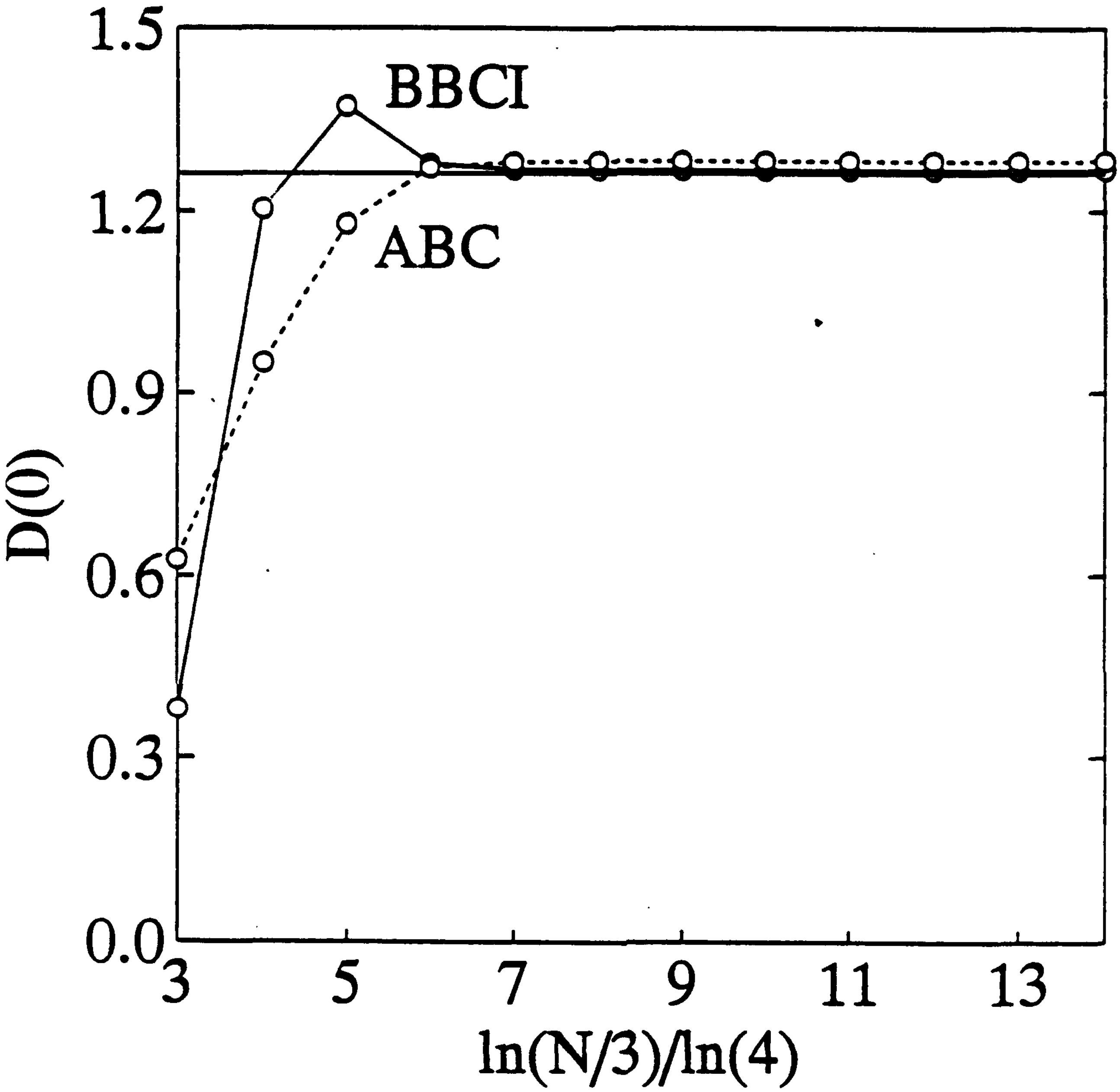

Figure 2(c). q = 0.

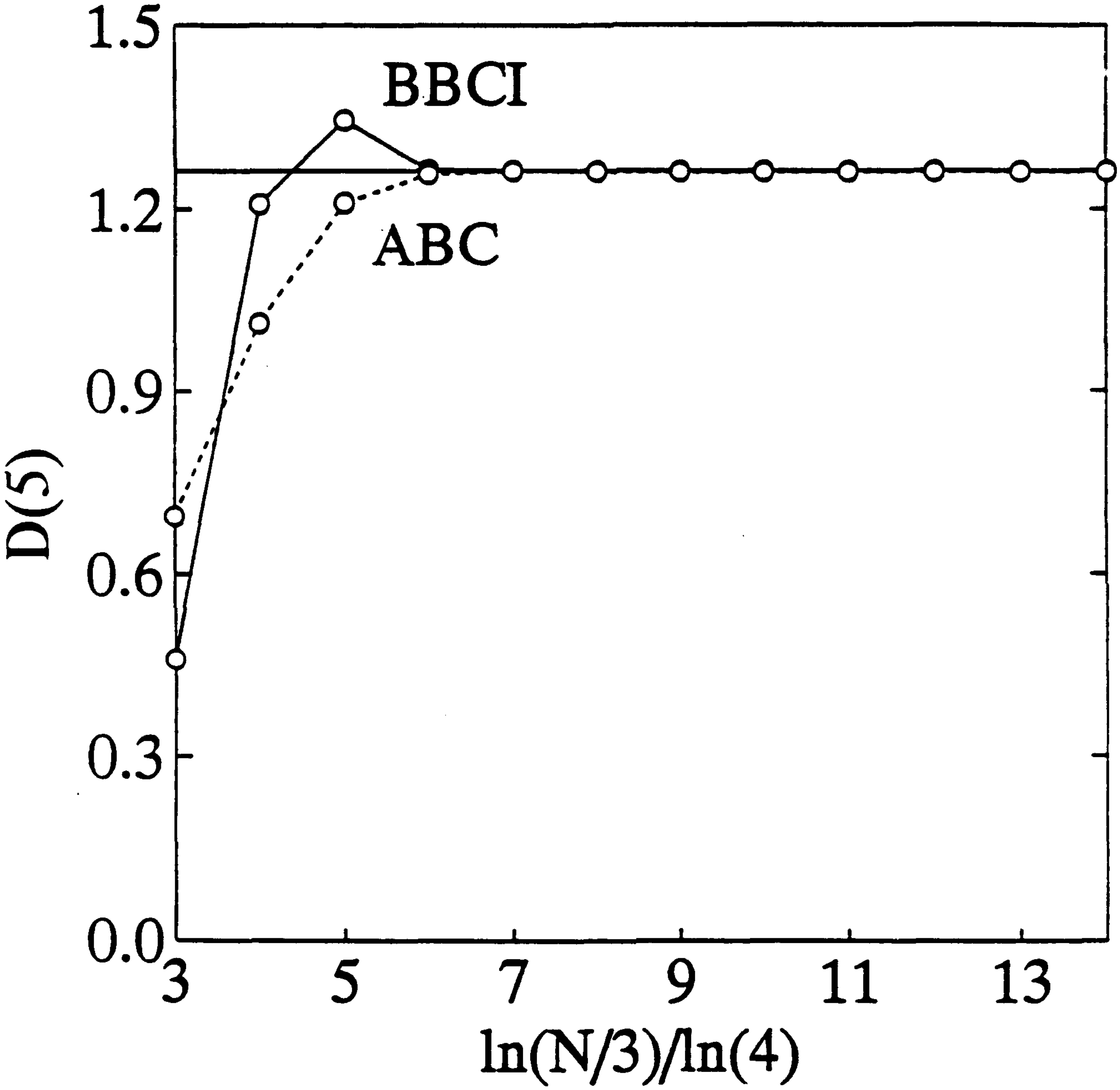

Figure 2(d). q = 5.

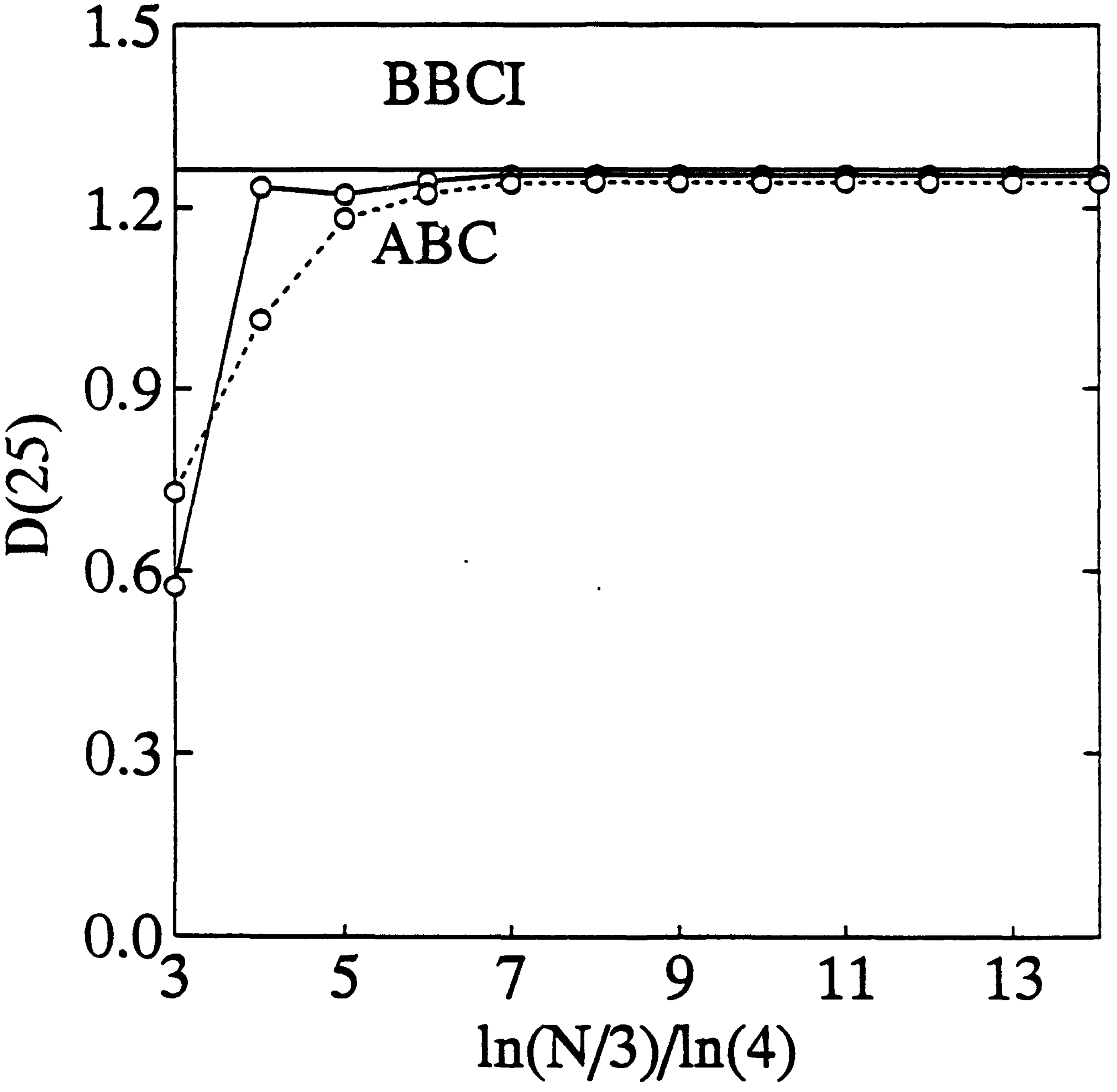

Figure 2(e). q = 25.

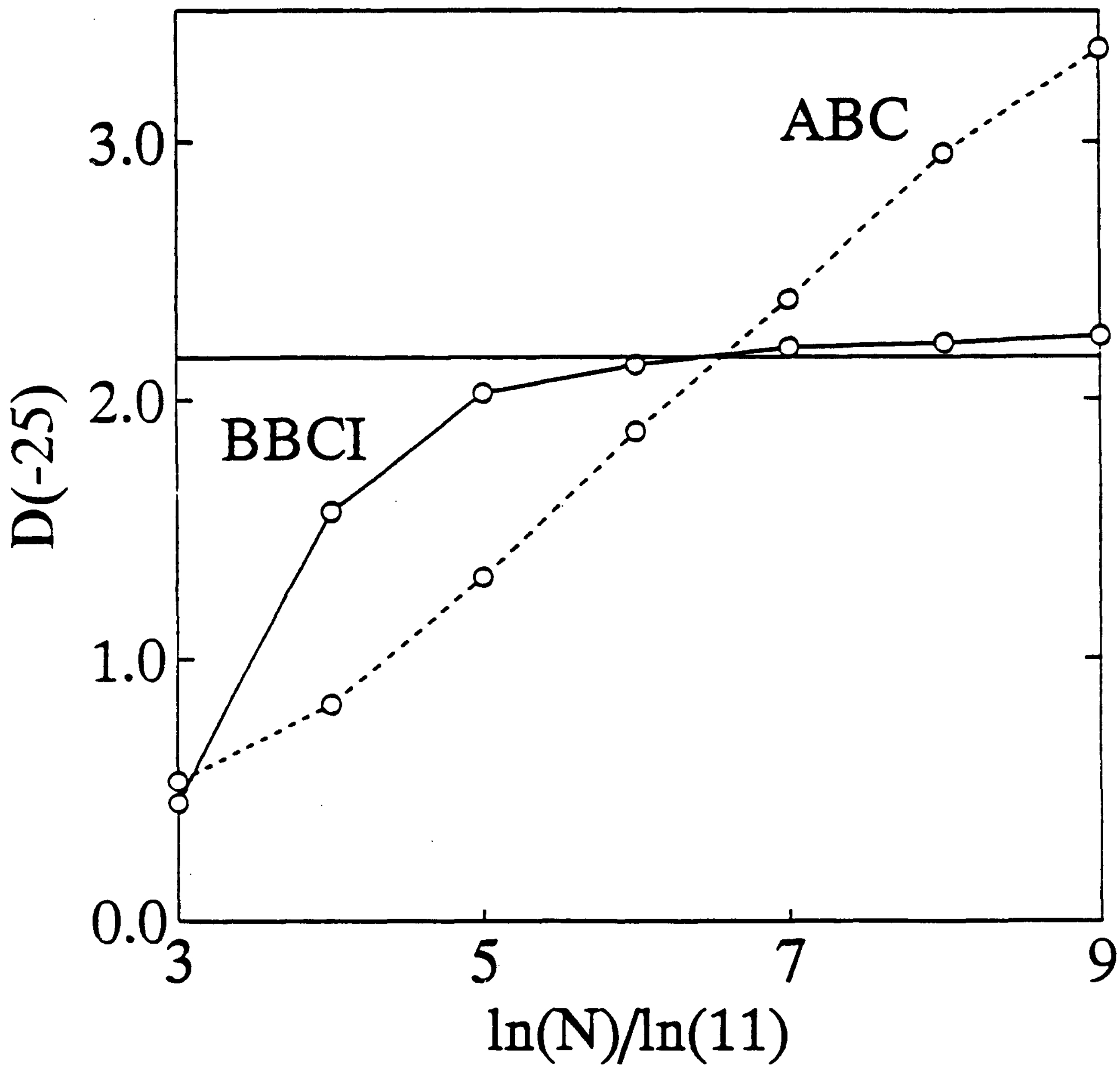

Figure 3. Hentschell and Procaccia generalized dimension D(q) versus normalized logarithm of the number of points in the fractal subset for split snowflake halls (ref 7).

(a). q = -25.

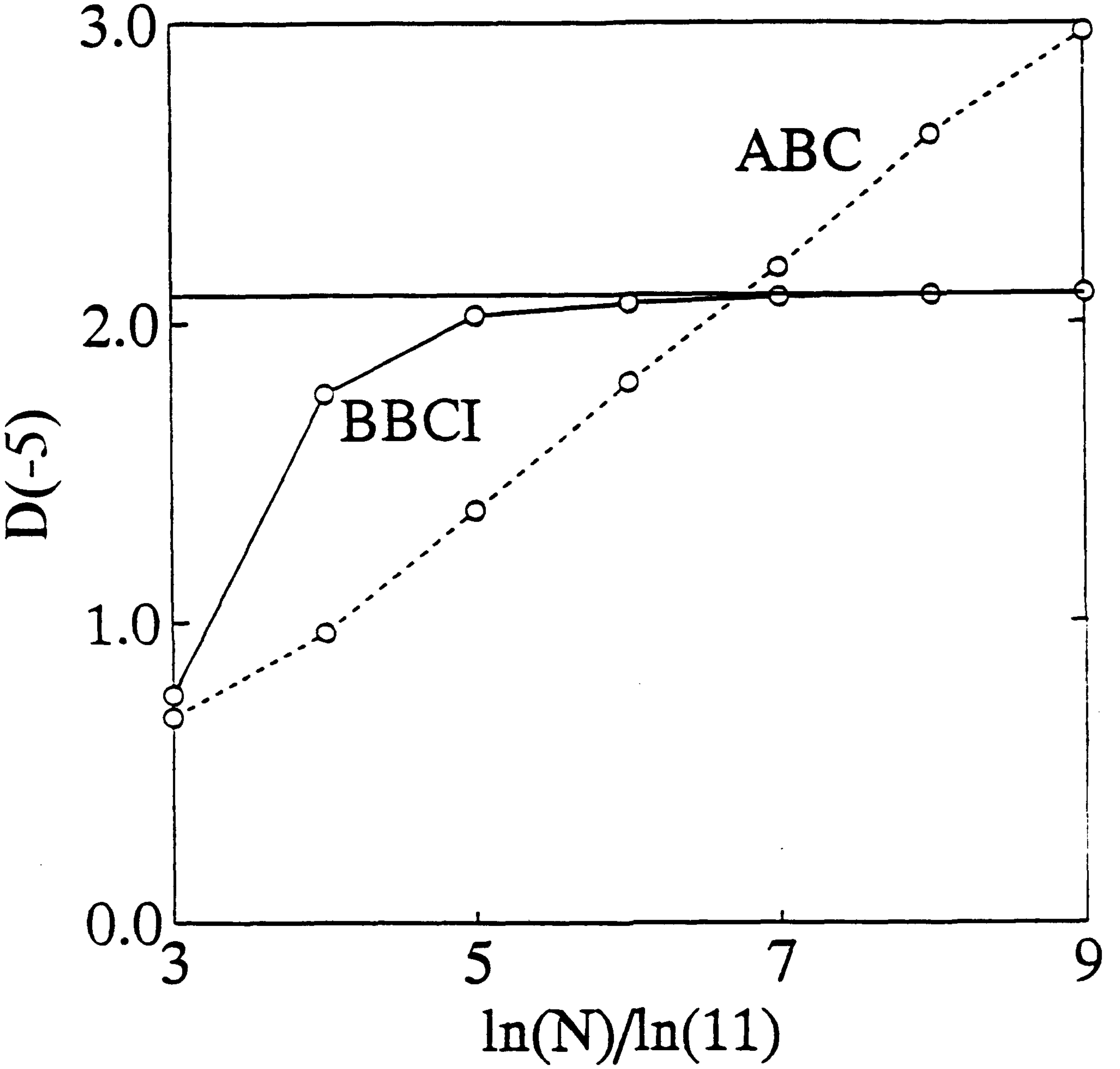

Figure 3(b). $q = -5$.

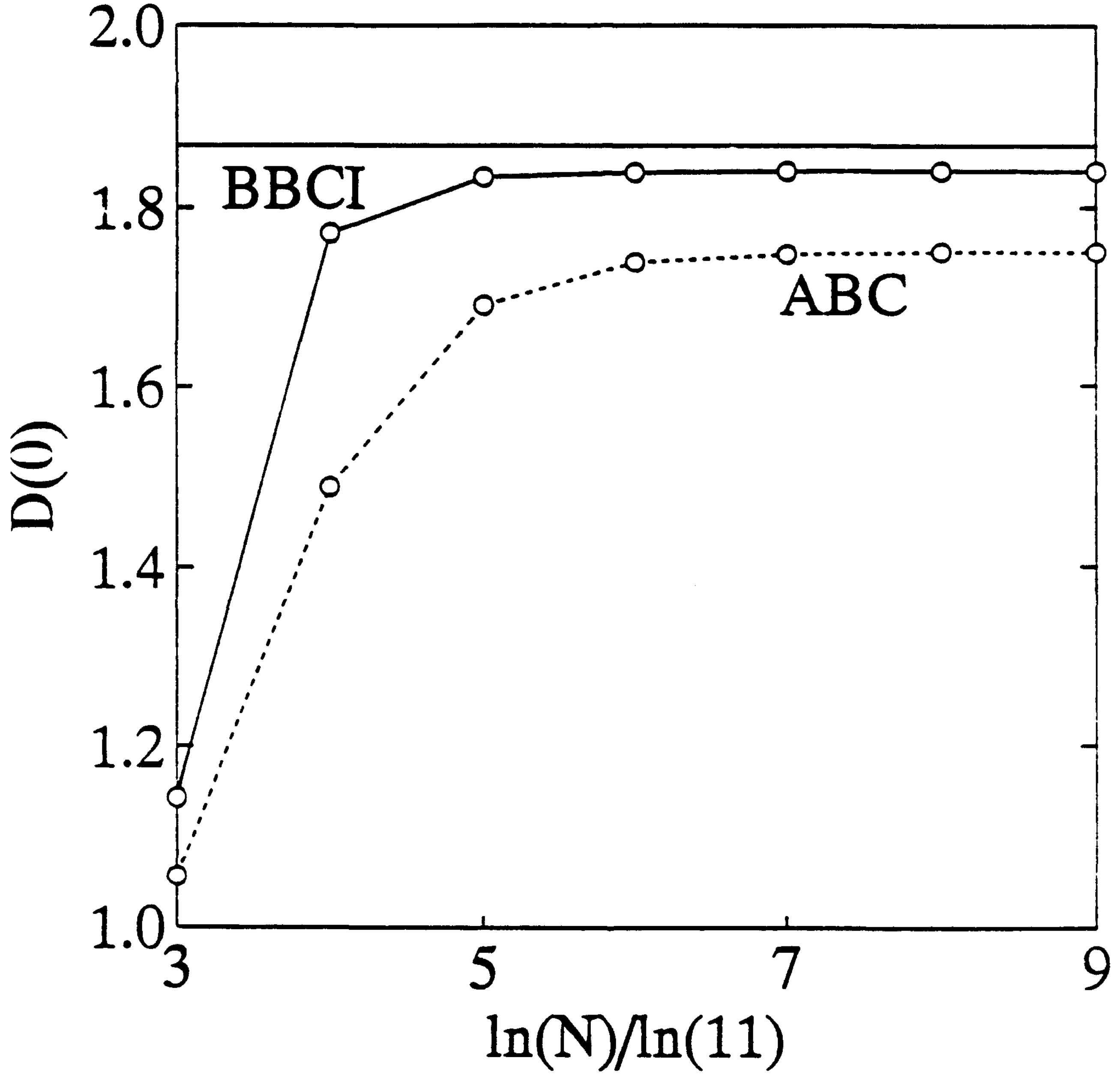

Figure 3(c). $q = 0$.

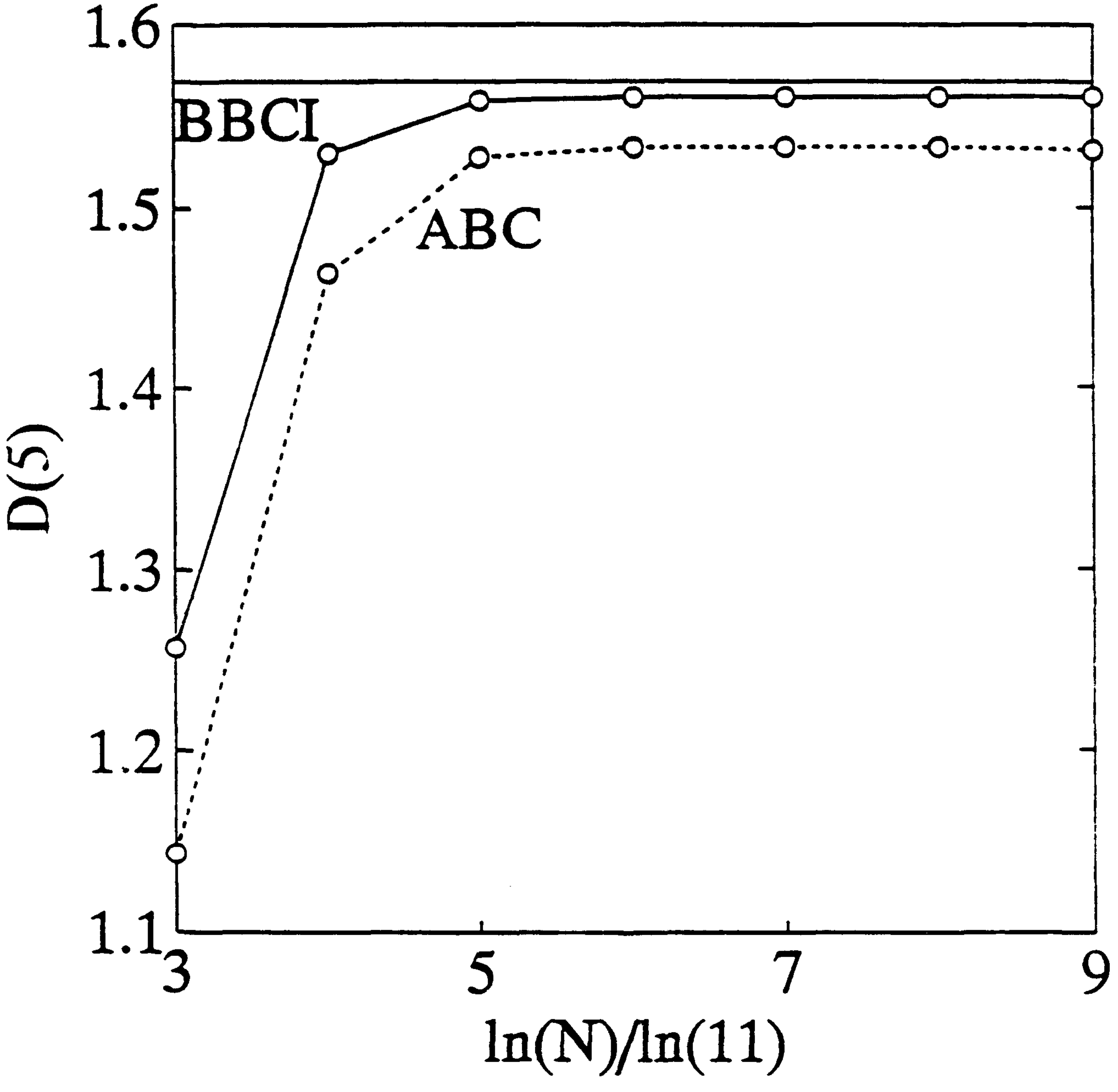

Figure 3(d). q = 5.

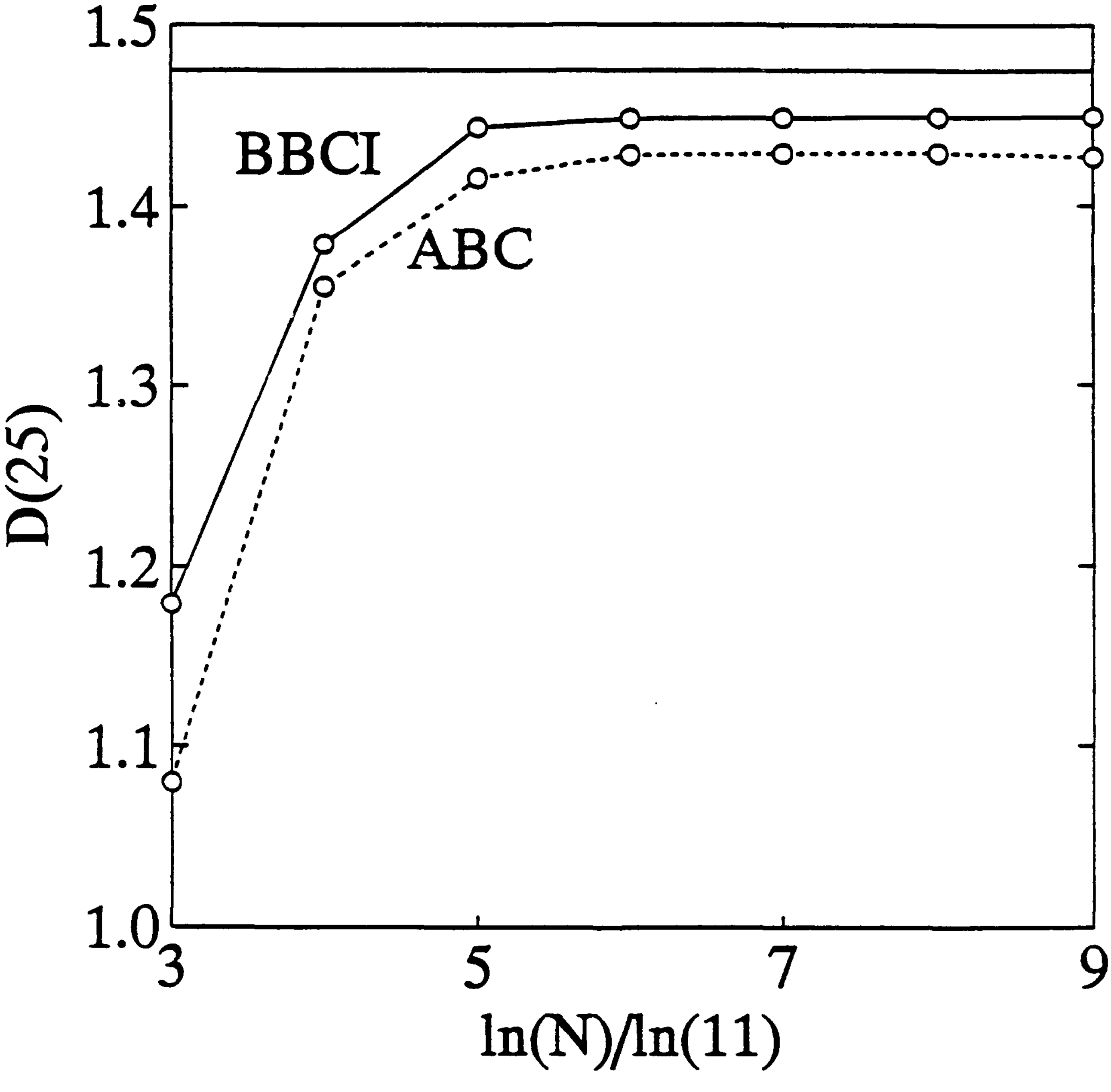

Figure 3(e). q = 25.

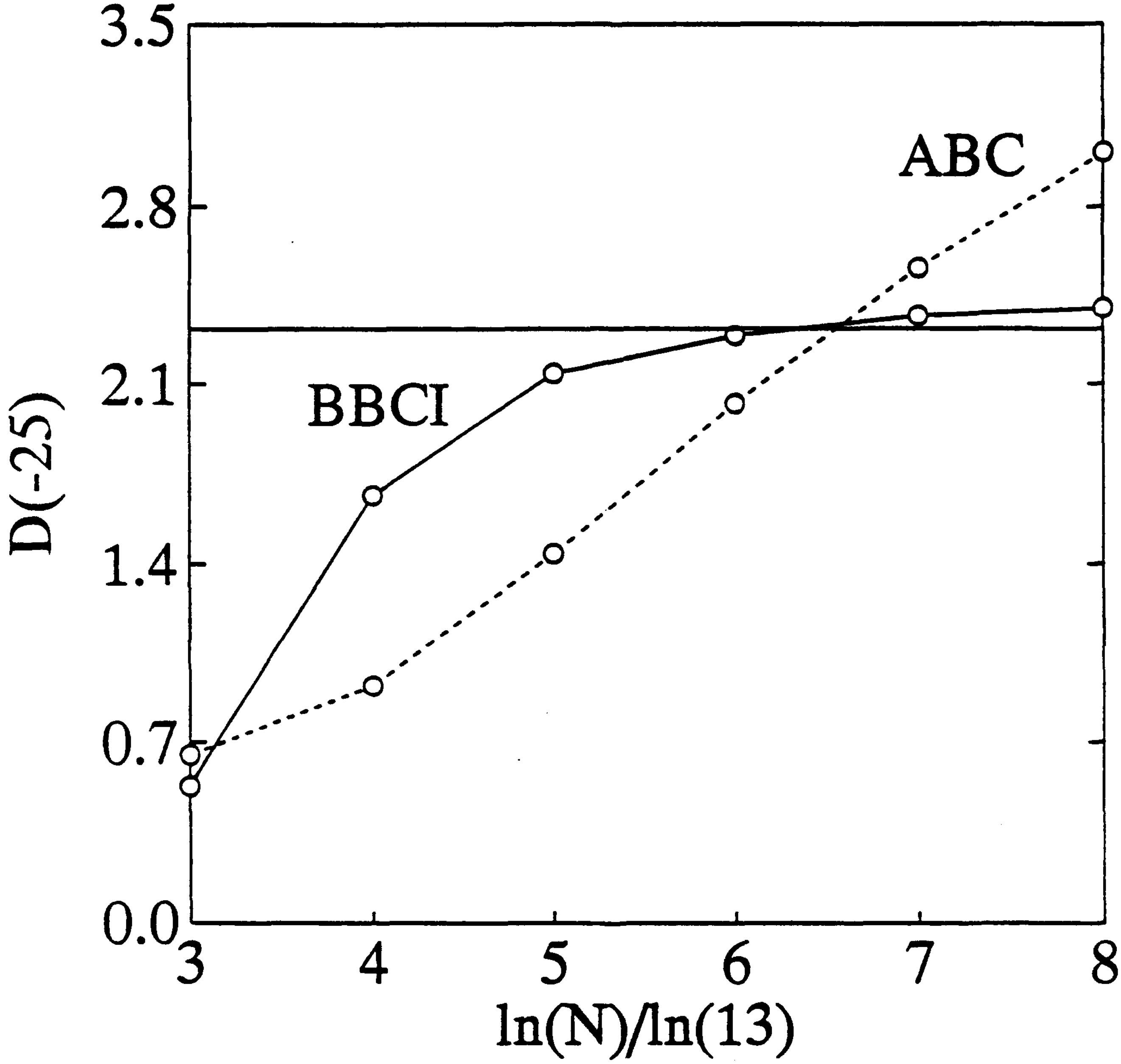

Figure 4. Hentschell and Procaccia generalized dimension D(q) versus normalized logarithm of the number of points in the fractal subset for the 13 element generator construction (ref 8).

(a). q = -25.

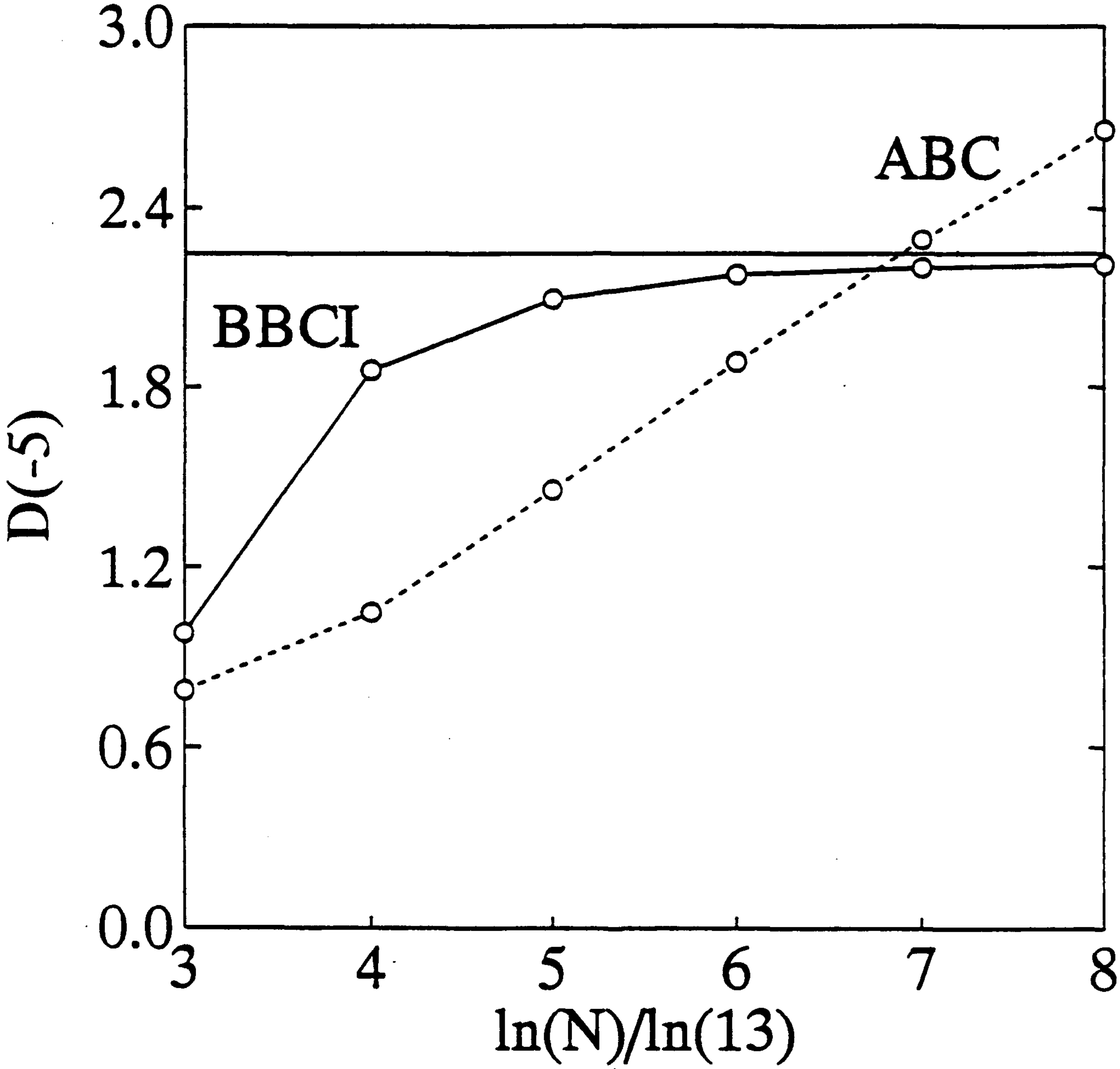

Figure 4(b). q = -5.

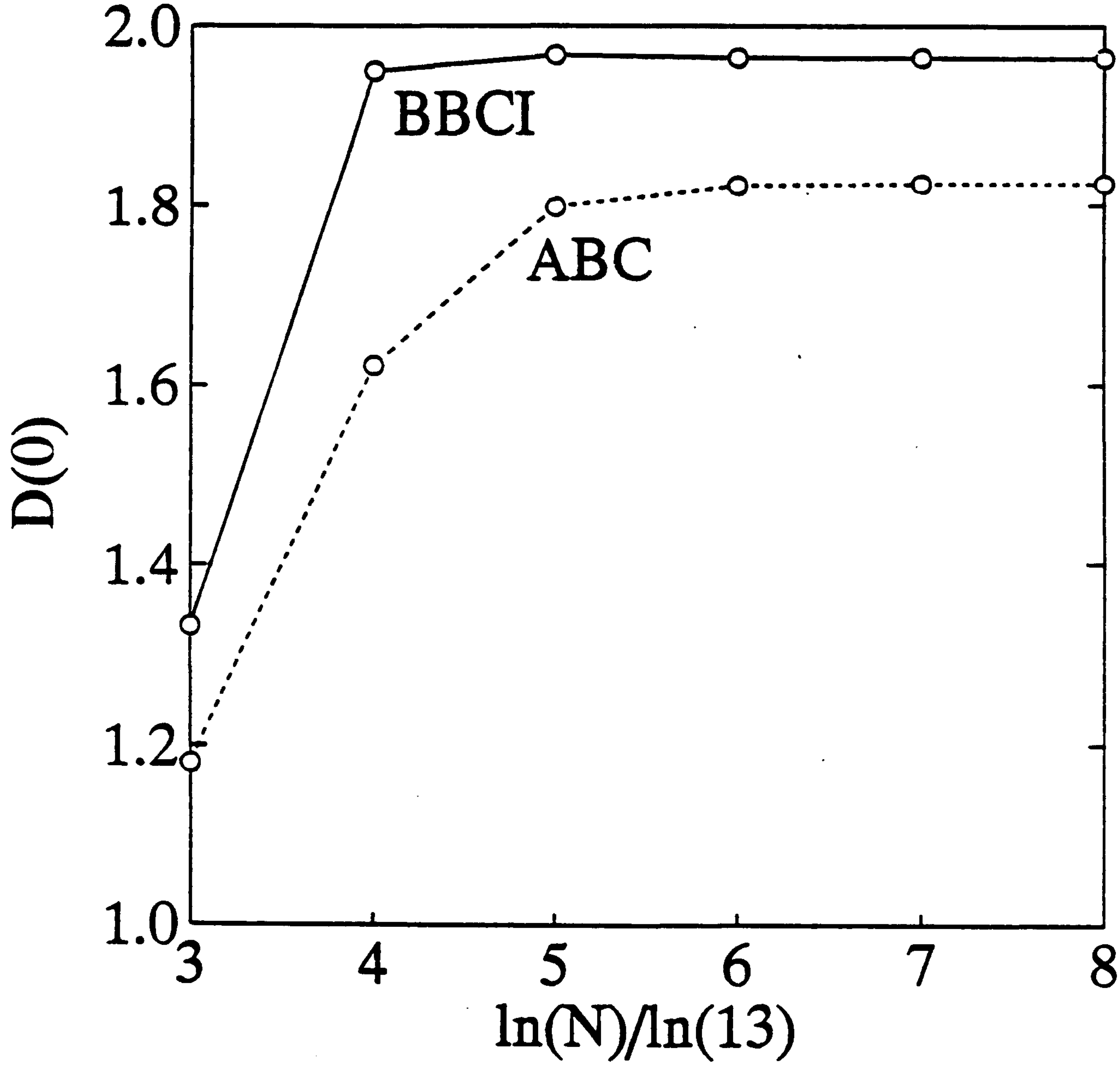

Figure 4(c). q = 0.

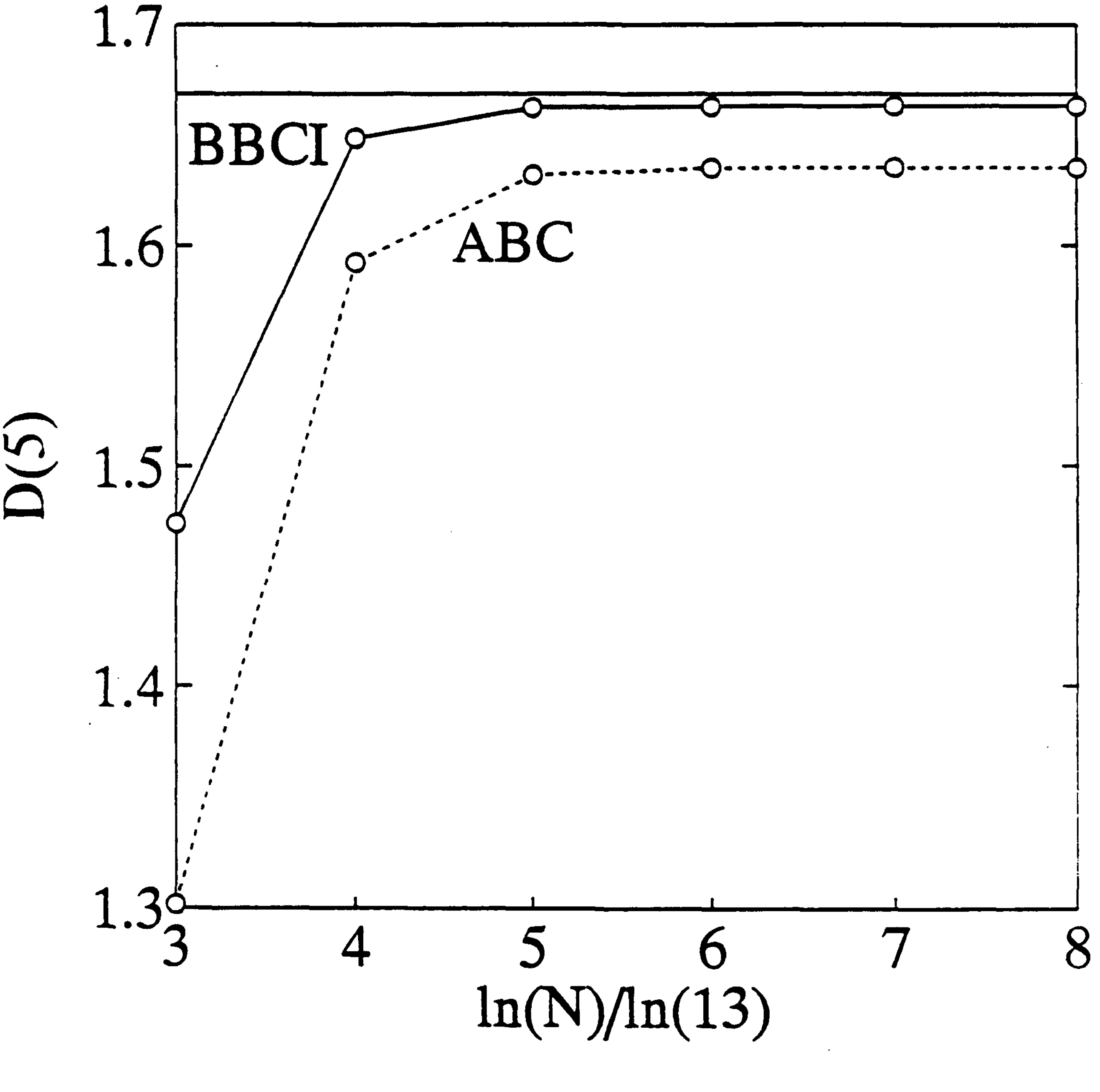

Figure 4(d). q = 5.

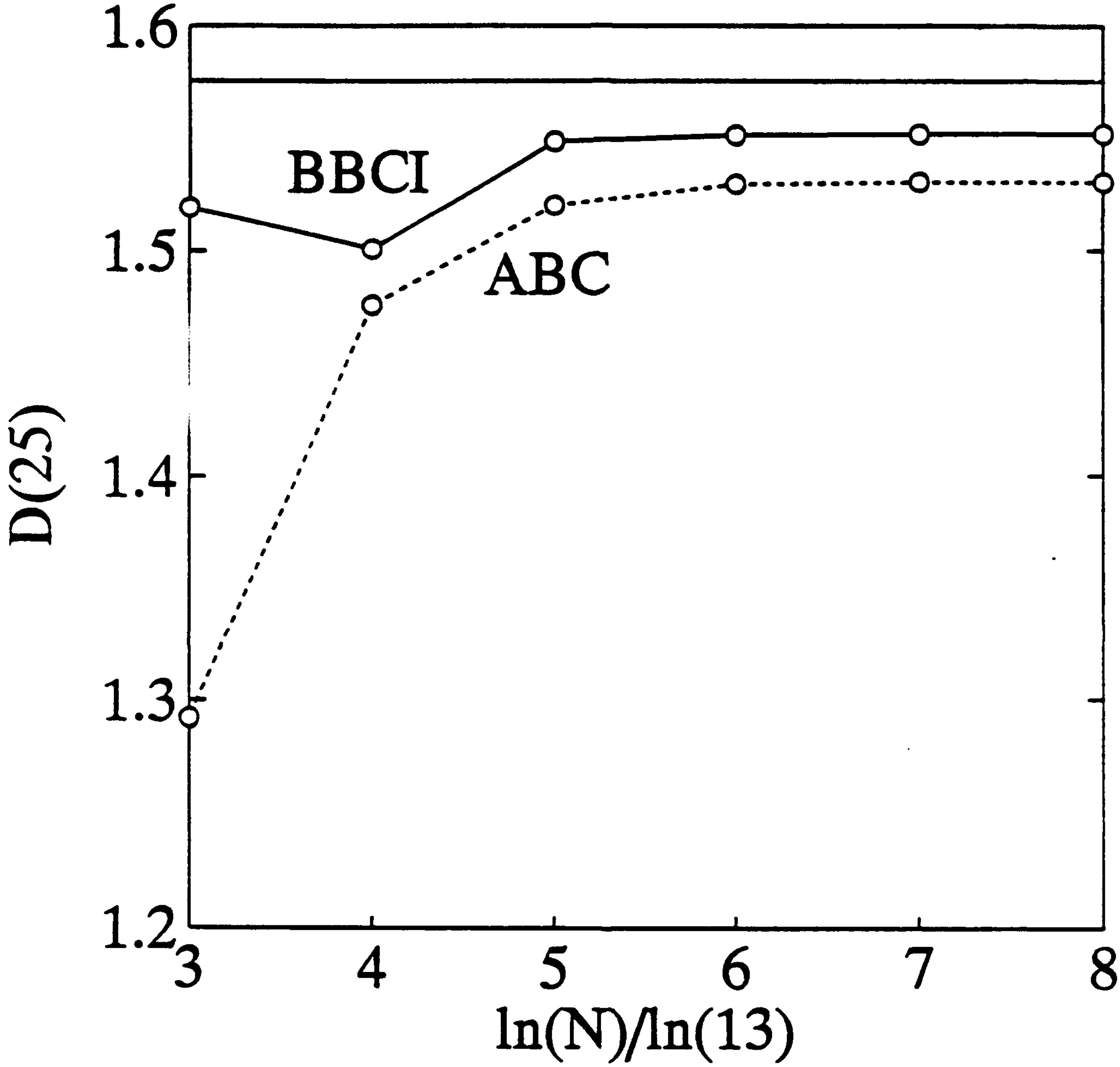

Figure 4(e). q = 25.

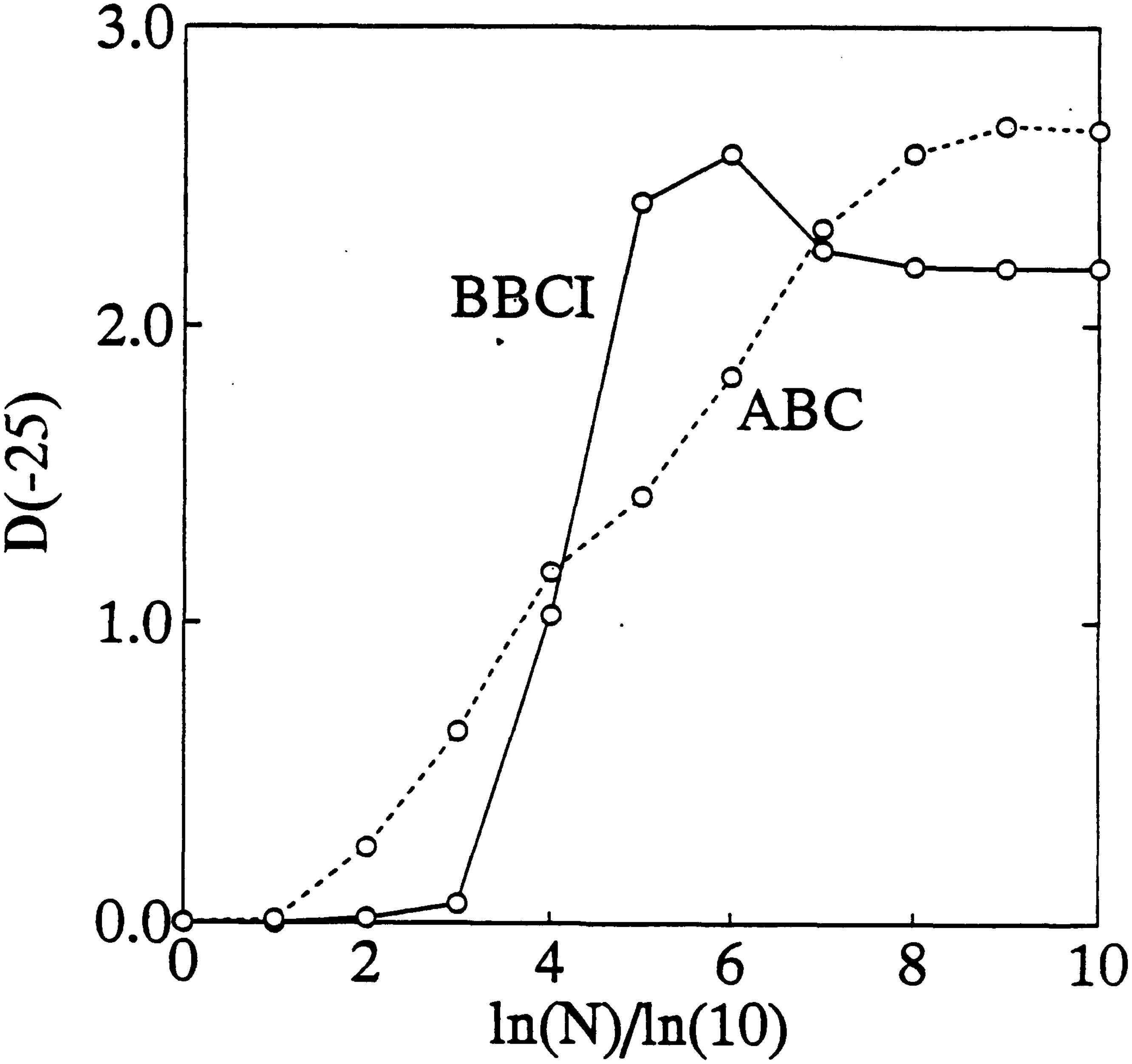

Figure 5. Hentschell and Procaccia generalized dimension D(q) versus normalized logarithm of the number of points in the fractal subset for the attractor for the symmetric chaotic mapping of Figure 3(a) of Reference 9.

(a). q = -25.

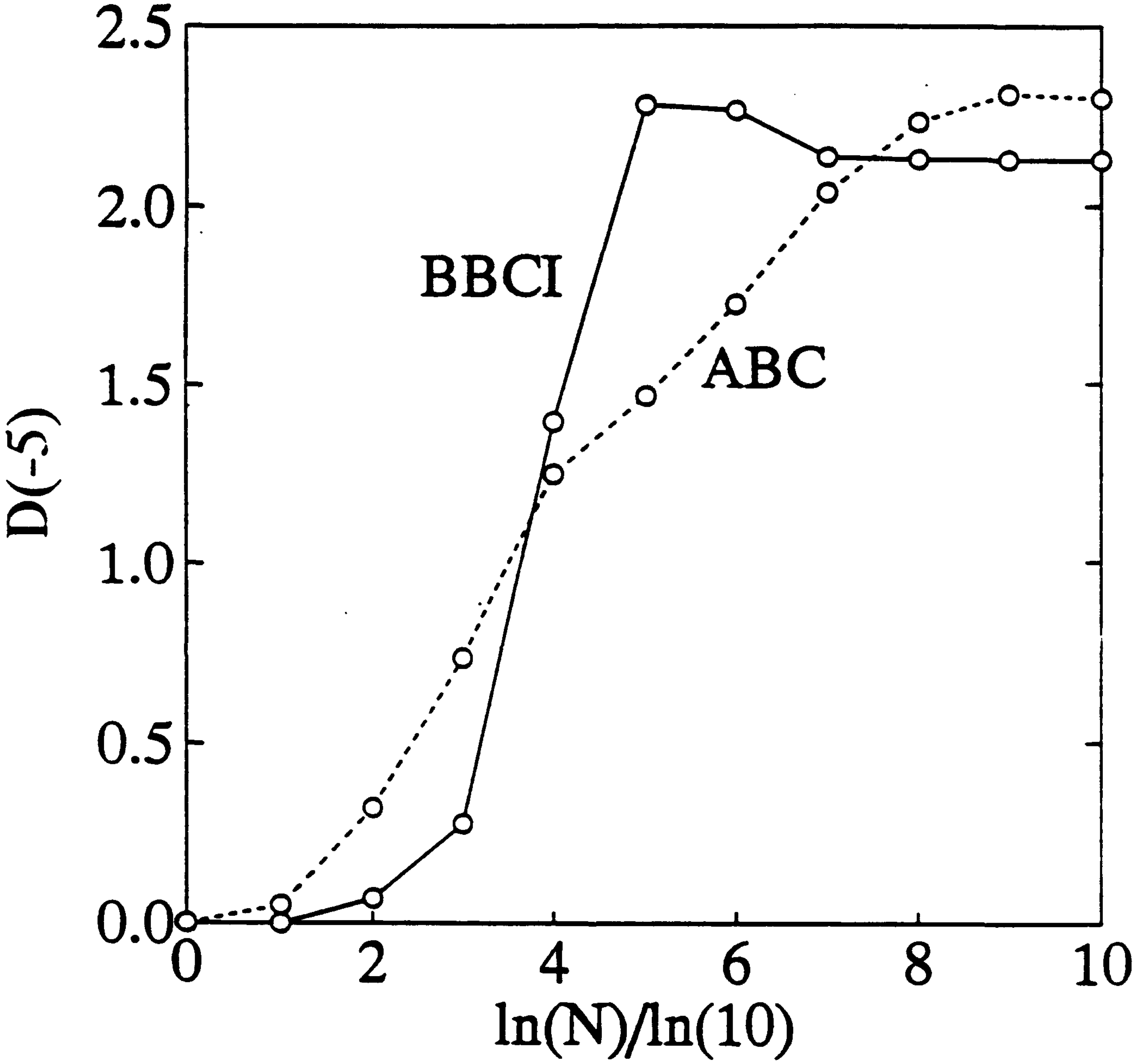

Figure 5(b). q = -5.

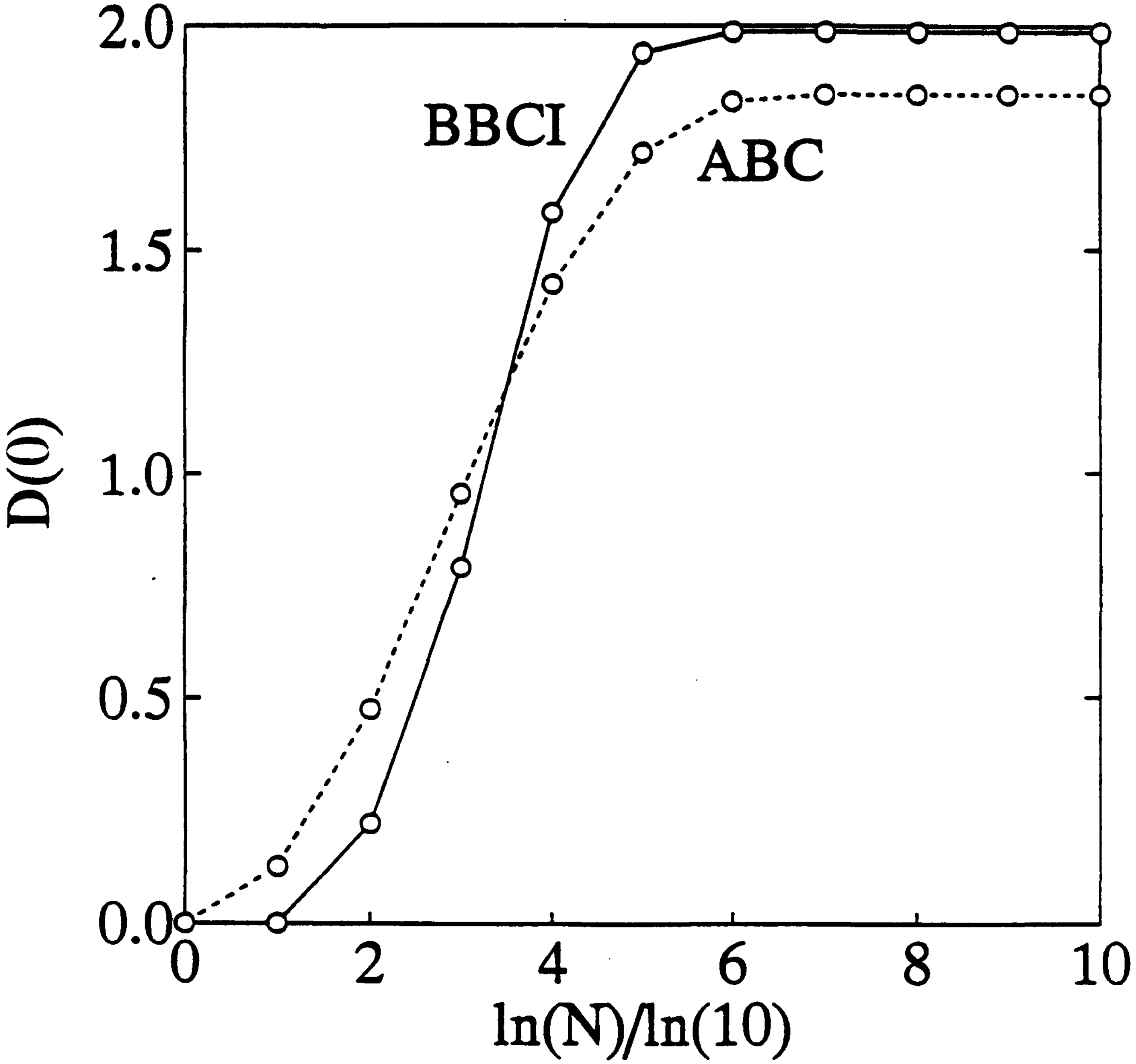

Figure 5(c). q = 0.

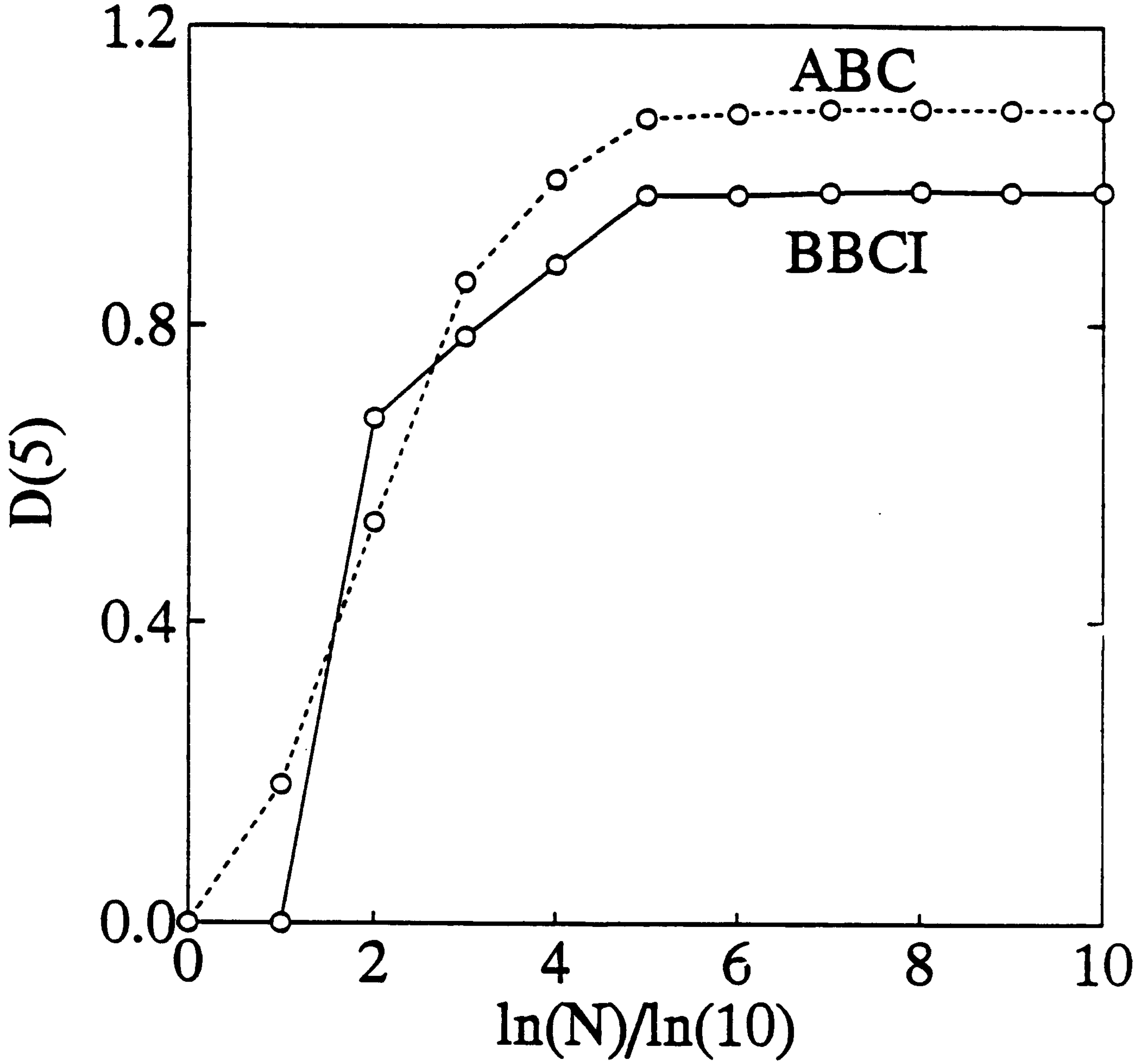

Figure 5(d). q = 5.

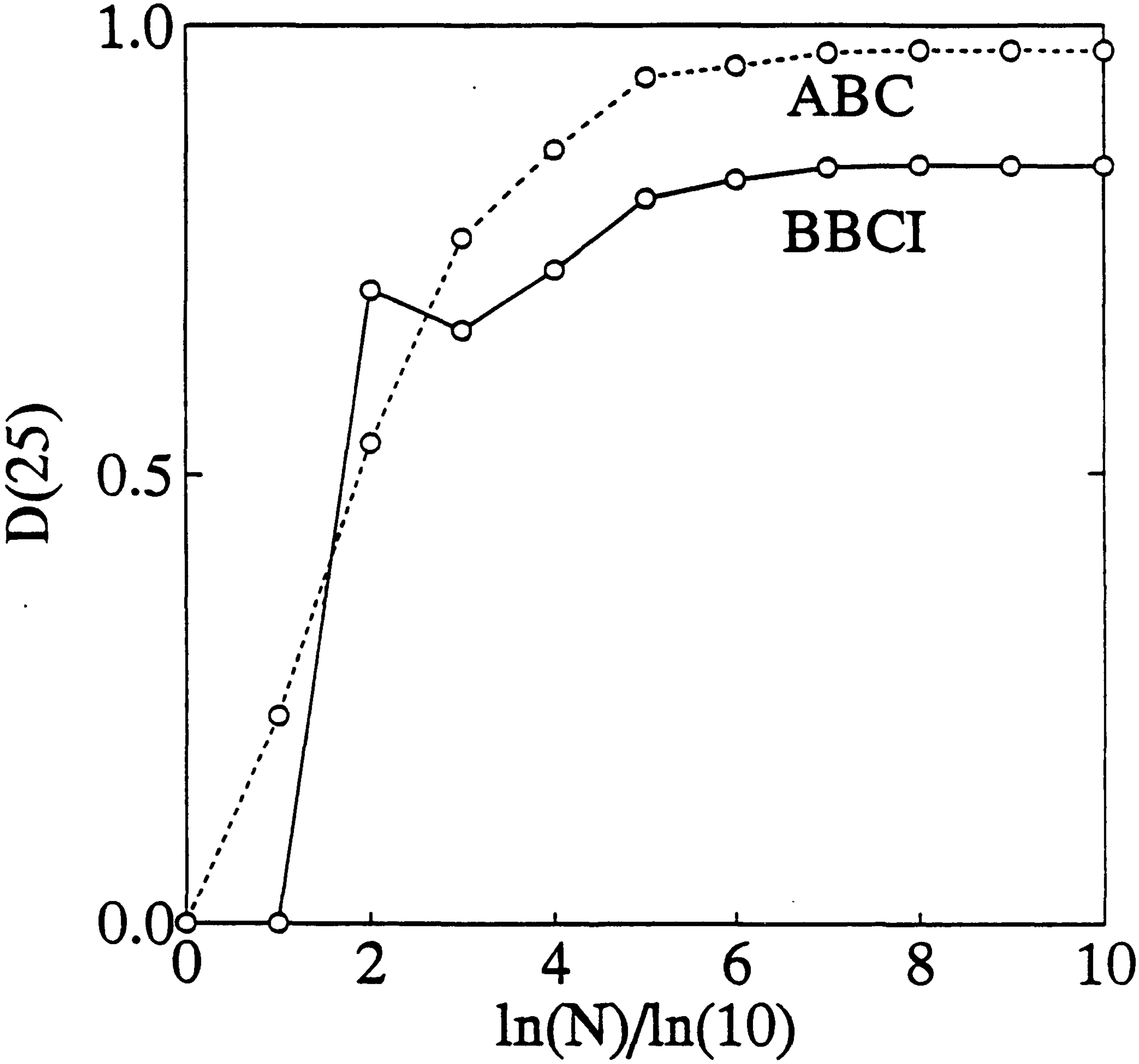

Figure 5(e). q = 25.

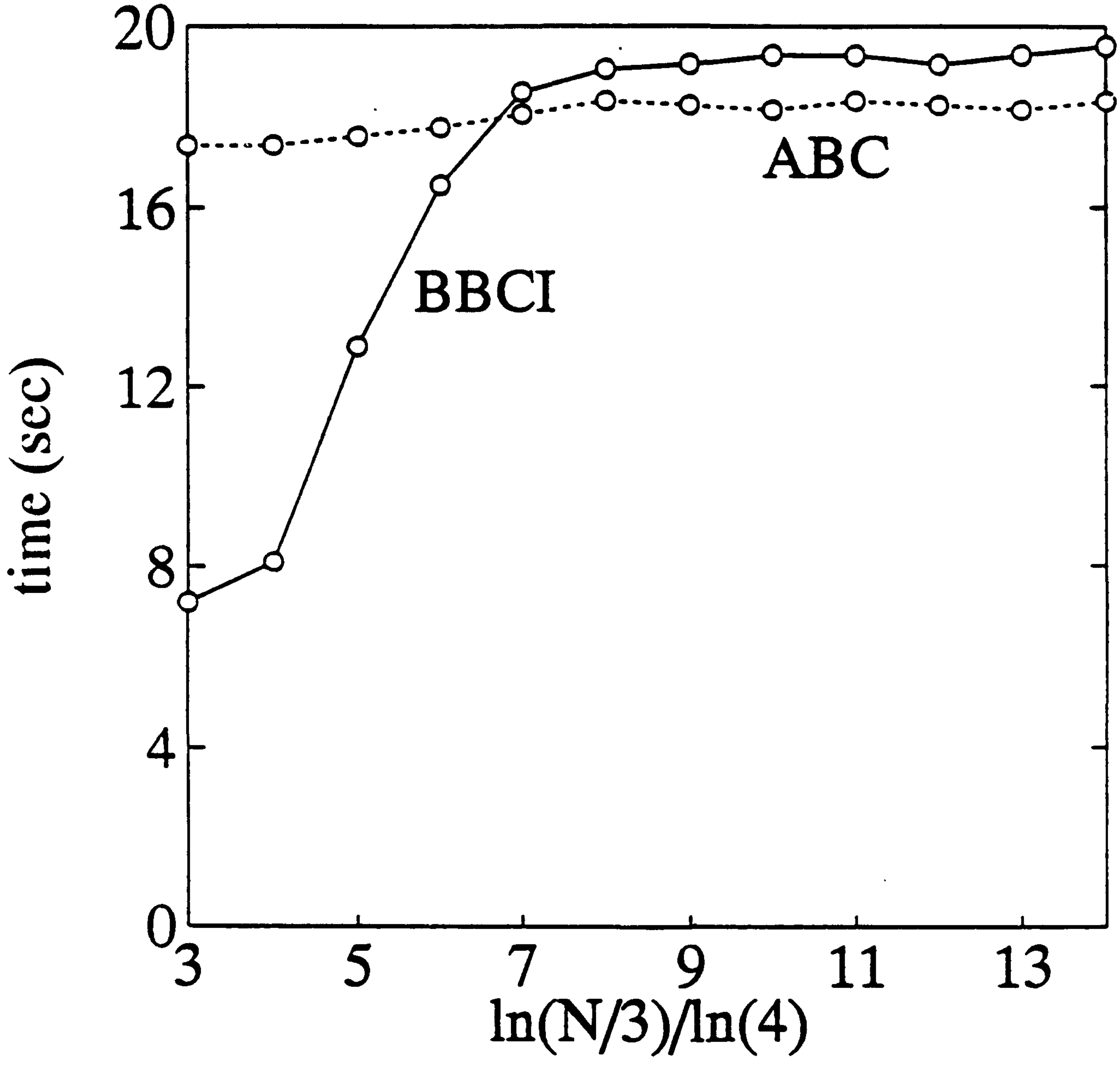

Figure 6. Cpu time versus normalized logarithm of the number of points in the fractal subsets.

(a). Asymmetric [0.4,0.2] triadic snowflake.

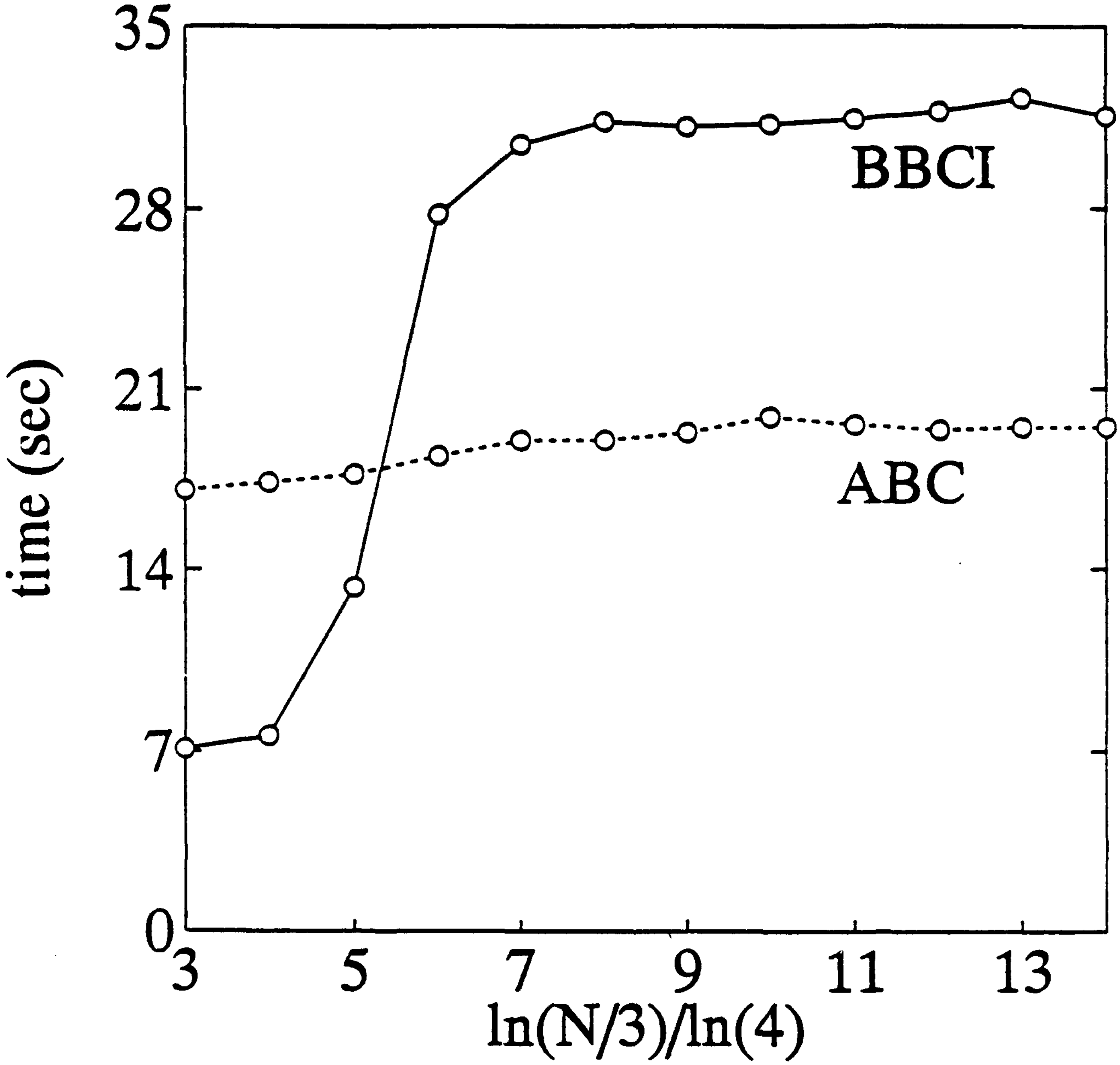

Figure 6(b). Koch triadic snowflake.

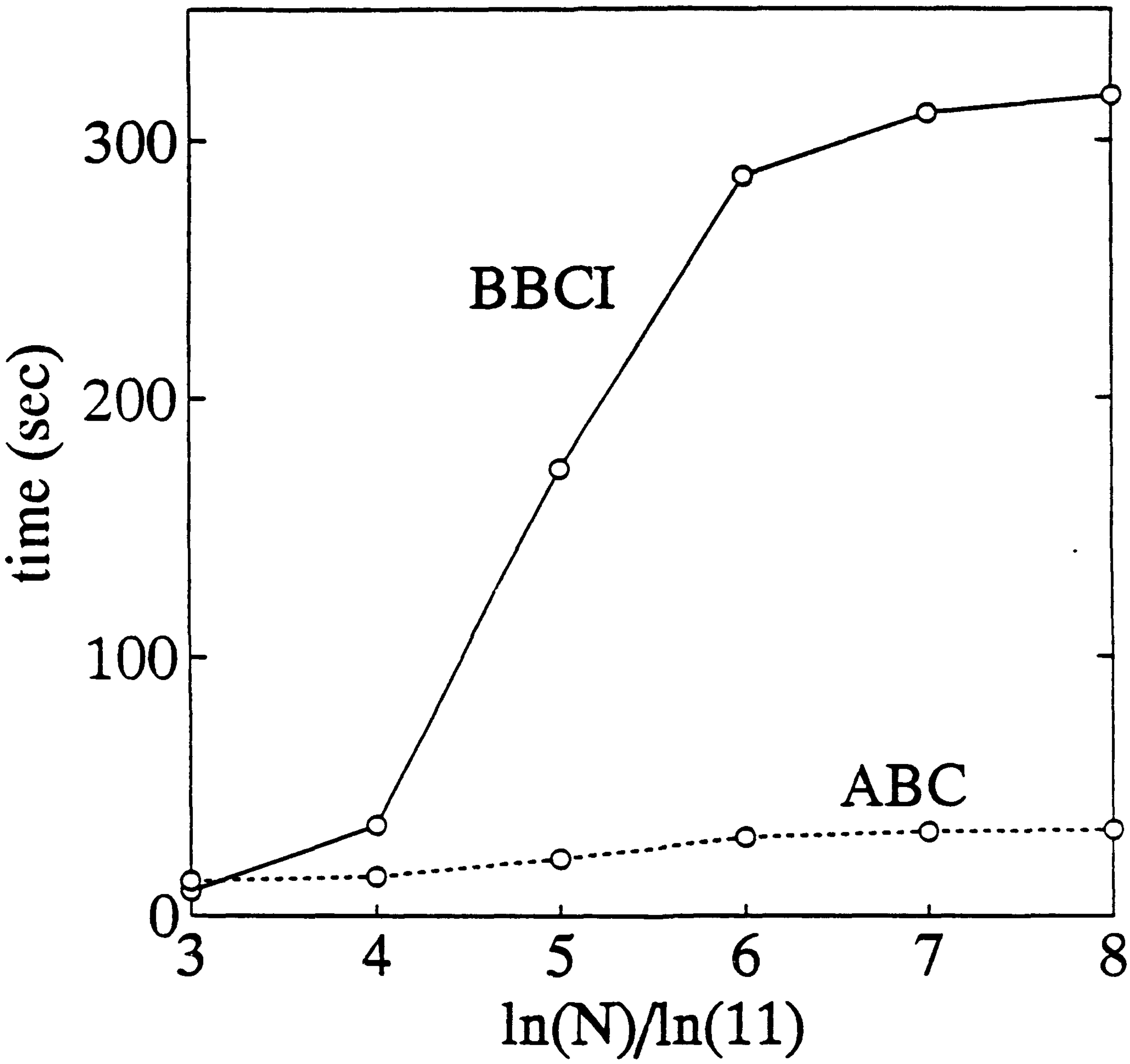

Figure 6(c). Split snowflake halls.

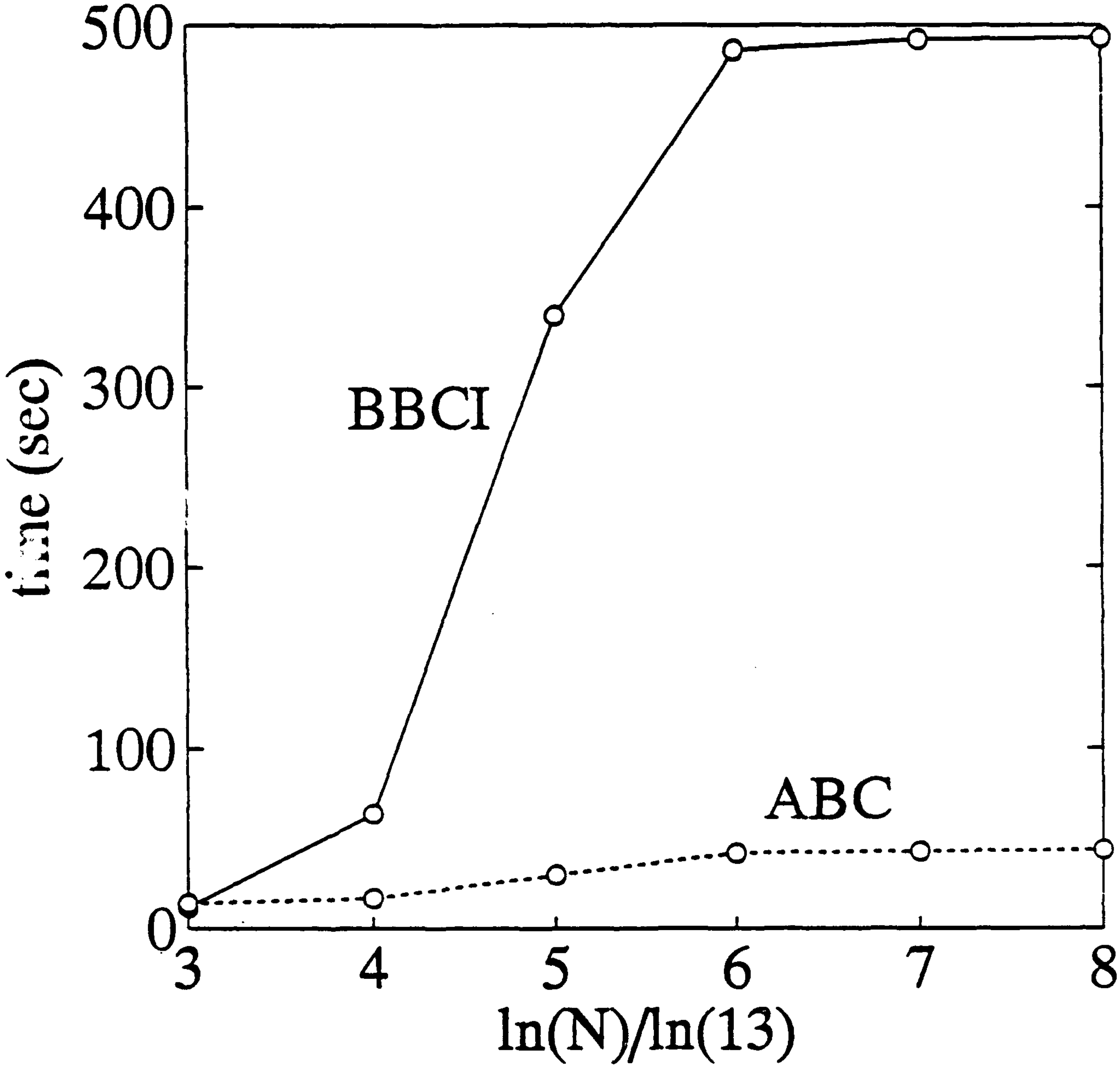

Figure 6(d). Mandelbrot's construction based on a 13 element generator (ref 8).

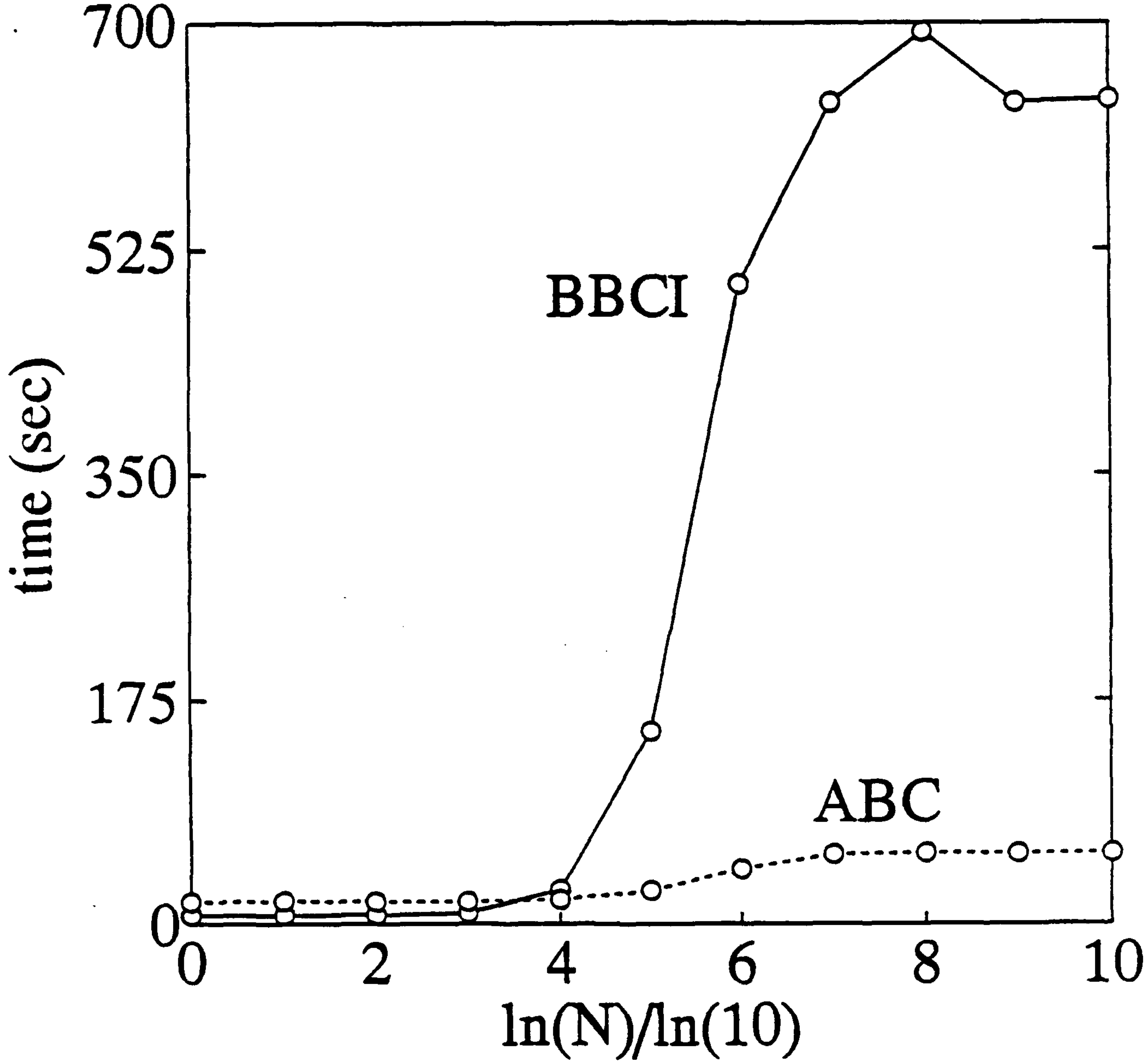

Figure 6(e). The D6 symmetric chaotic mapping of Figure 3a of Reference 9.

TECHNICAL REPORT INTERNAL DISTRIBUTION LIST

	NO. OF COPIES
CHIEF, DEVELOPMENT ENGINEERING DIVISION	
ATTN: SMCAR-CCB-DA	1
-DC	1
-DI	1
-DR	1
-DS (SYSTEMS)	1
CHIEF, ENGINEERING DIVISION	
ATTN: SMCAR-CCB-S	1
-SD	1
-SE	1
CHIEF, RESEARCH DIVISION	
ATTN: SMCAR-CCB-R	2
-RA	1
-RE	1
-RM	1
-RP	1
-RT	1
TECHNICAL LIBRARY	
ATTN: SMCAR-CCB-TL	5
TECHNICAL PUBLICATIONS & EDITING SECTION	
ATTN: SMCAR-CCB-TL	3
OPERATIONS DIRECTORATE	
ATTN: SMCWV-ODP-P	1
DIRECTOR, PROCUREMENT & CONTRACTING DIRECTORATE	
ATTN: SMCWV-PP	1
DIRECTOR, PRODUCT ASSURANCE & TEST DIRECTORATE	
ATTN: SMCWV-QA	1

NOTE: PLEASE NOTIFY DIRECTOR, BENÉT LABORATORIES, ATTN: SMCAR-CCB-TL OF ADDRESS CHANGES.

TECHNICAL REPORT EXTERNAL DISTRIBUTION LIST

	NO. OF COPIES
ASST SEC OF THE ARMY RESEARCH AND DEVELOPMENT ATTN: DEPT FOR SCI AND TECH THE PENTAGON WASHINGTON, D.C. 20310-0103	1
ADMINISTRATOR DEFENSE TECHNICAL INFO CENTER ATTN: DTIC-FDAC CAMERON STATION ALEXANDRIA, VA 22304-6145	12
COMMANDER U.S. ARMY ARDEC	
ATTN: SMCAR-AEE	1
SMCAR-AES, BLDG. 321	1
SMCAR-AET-O, BLDG. 351N	1
SMCAR-CC	1
SMCAR-FSA	1
SMCAR-FSM-E	1
SMCAR-FSS-D, BLDG. 94	1
SMCAR-IMI-I, (STINFO) BLDG. 59	2
PICATINNY ARSENAL, NJ 07806-5000	
DIRECTOR U.S. ARMY RESEARCH LABORATORY ATTN: AMSRL-DD-T, BLDG. 305 ABERDEEN PROVING GROUND, MD 21005-5066	1
DIRECTOR U.S. ARMY RESEARCH LABORATORY ATTN: AMSRL-WT-PD (DR. B. BURNS) ABERDEEN PROVING GROUND, MD 21005-5066	1
DIRECTOR U.S. MATERIEL SYSTEMS ANALYSIS ACTV ATTN: AMXSY-MP ABERDEEN PROVING GROUND, MD 21005-5071	1
COMMANDER ROCK ISLAND ARSENAL ATTN: SMCRI-ENM ROCK ISLAND, IL 61299-5000	1
MIAC/CINDAS PURDUE UNIVERSITY P.O. BOX 2634 WEST LAFAYETTE, IN 47906	1
COMMANDER U.S. ARMY TANK-AUTMV R&D COMMAND ATTN: AMSTA-DDL (TECH LIBRARY) WARREN, MI 48397-5000	1
COMMANDER U.S. MILITARY ACADEMY ATTN: DEPARTMENT OF MECHANICS WEST POINT, NY 10966-1792	1
U.S. ARMY MISSILE COMMAND REDSTONE SCIENTIFIC INFO CENTER ATTN: DOCUMENTS SECTION, BLDG. 4484 REDSTONE ARSENAL, AL 35898-5241	2
COMMANDER U.S. ARMY FOREIGN SCI & TECH CENTER ATTN: DRXST-SD 220 7TH STREET, N.E. CHARLOTTESVILLE, VA 22901	1
COMMANDER U.S. ARMY LABCOM MATERIALS TECHNOLOGY LABORATORY ATTN: SLCMT-IML (TECH LIBRARY) WATERTOWN, MA 02172-0001	2
COMMANDER U.S. ARMY LABCOM, ISA ATTN: SLCIS-IM-TL 2800 POWER MILL ROAD ADELPHI, MD 20783-1145	1

NOTE: PLEASE NOTIFY COMMANDER, ARMAMENT RESEARCH, DEVELOPMENT, AND ENGINEERING CENTER, U.S. ARMY AMCCOM, ATTN: BENÉT LABORATORIES, SMCAR-CCB-TL, WATERVLIET, NY 12189-4050 OF ADDRESS CHANGES.

TECHNICAL REPORT EXTERNAL DISTRIBUTION LIST (CONT'D)

	NO. OF COPIES
COMMANDER U.S. ARMY RESEARCH OFFICE ATTN: CHIEF, IPO P.O. BOX 12211 RESEARCH TRIANGLE PARK, NC 27709-2211	1
DIRECTOR U.S. NAVAL RESEARCH LABORATORY ATTN: MATERIALS SCI & TECH DIV CODE 26-27 (DOC LIBRARY) WASHINGTON, D.C. 20375	1 1
COMMANDER AIR FORCE ARMAMENT LABORATORY ATTN: AFATL/MN EGLIN AFB, FL 32542-5434	1
COMMANDER AIR FORCE ARMAMENT LABORATORY ATTN: AFATL/MNF EGLIN AFB, FL 32542-5434	1

NOTE: PLEASE NOTIFY COMMANDER, ARMAMENT RESEARCH, DEVELOPMENT, AND ENGINEERING CENTER, U.S. ARMY AMCCOM, ATTN: BENÉT LABORATORIES, SMCAR-CCB-TL, WATERVLIET, NY 12189-4050 OF ADDRESS CHANGES.